Geochemical Thermometry of Rocks of the Talnakh Intrusion: Assessment of the Melt Composition and the Crystallinity of the Parental Magma

Article *in* Petrology · September 2001

CITATIONS
35

READS
82

4 authors, including:

Nadezhda Krivolutskaya
Russian Academy of Sciences
123 PUBLICATIONS **2,478** CITATIONS

SEE PROFILE

Alexey Ariskin
Lomonosov Moscow State University
249 PUBLICATIONS **2,155** CITATIONS

SEE PROFILE

Petrology, Vol. 9, No. 5, 2001, pp. 389–414. Translated from Petrologiya, Vol. 9, No. 5, 2001, pp. 451–479.

Geochemical Thermometry of Rocks of the Talnakh Intrusion: Assessment of the Melt Composition and the Crystallinity of the Parental Magma

N. A. Krivolutskaya *, A. A. Ariskin **, S. F. Sluzhenikin *, and D. M. Turovtsev *

** Institute of the Geology of Ore Deposits, Petrography, Mineralogy, and Geochemistry, Russian Academy of Sciences, Staromonetnyi per. 35, Moscow, 109017 Russia*
e-mail: nakriv@mail.ru

*** Vernadsky Institute of Geochemistry and Analytical Chemistry, Russian Academy of Sciences, ul. Kosygina 19, Moscow, 117975 Russia*

Received December 1, 2000

Abstract—Techniques of geochemical thermometry with the use of the COMAGMAT computer program were utilized to assay the phase and chemical composition of the parental magma of the Talnakh intrusion and the melt–crystal mixtures that produced the taxitic and picritic gabbro-dolerites of the lower zone of the massif. These results point to the cotectic (*Ol* + *Pl*) composition of the Talnakh magma, which was intruded at a temperature of approximately 1200°C and contained 10–15% intratelluric phenocrysts, predominantly *Ol* (7–11%). The composition of the parental magmatic melt (the liquid constituent of the magma) corresponded to tholeiitic ferrobasalt with somewhat higher concentrations of MgO (~8 wt %) and K_2O (~0.7 wt %) than in the "normal" flood basalts in the Siberian Platform. This composition was determined to be analogous to the composition of the residual liquids, which are preserved as intercumulus material in the rocks of the taxitic and picritic units. The compositional variations of rocks in the lower part of the Talnakh intrusion are explained as resulting from variations in the proportions of intratelluric *Ol* and *Pl* crystals and the intercumulus liquid. This validates the conclusion that the taxitic and picritic gabbro-dolerites were produced by a single parental magma of the tholeiitic type. The composition of its liquid can be quite well approximated by that of the contact gabbro-dolerites. The calculated melt composition is close to that of the tholeiitic basalts of the late stage of flood-basalt magmatism in the Siberian Platform (Mokulaevskaya Formation).

INTRODUCTION

The genesis of sulfide and PGE mineralization in the ultramafic–mafic intrusions of the Noril'sk mining district are discussed in the literature over several decades. The occurrence of olivine-rich rocks and the related enrichment in Mg and higher Ni concentrations of the rocks led to the recognition of these massifs as a specific magnesian type of flood-basalt magmatism in the Siberian Platform (Godlevskii, 1959; Lur'e *et al.*, 1962; Dodin and Batuev, 1971; Nesterenko and Al'mukhamedov, 1973). At the same time, it remains uncertain as to why ore mineralization is associated only with intrusions of the Noril'sk type but not the rest of barren or poorly mineralized magmatic bodies. The principal factors that are commonly recognized as controlling the possibility of development of economic ore mineralization are as follows: (1) the composition of the parental melt; (2) magma segregation prior to its arrival at the chamber (including the fractional crystallization of the magmas and their contamination with crustal material); (3) processes of in-chamber differentiation, liquid immiscibility, and sulfide migration; (4) effect of fluids; and (5) structural, tectonic, and/or lithologic control (Godlevskii, 1959; Vilenskii, 1970; Zolotukhin, 1971, 1997; Likhachev, 1978, 1982; Zotov, 1979, 1989; Oleinikov, 1979; Distler *et al.*, 1988; Naldrett, 1992; Naldrett *et al.*, 1996). The importance of each of these factors for the genesis of ore mineralization and the conditions under which they can be realized extend beyond the scope of our study, and here we will focus on the more general problem of the magma source of the "normal" (i.e., relatively Fe-rich; Masaitis, 1958; Kutolin, 1972) and magnesian flood-basalt intrusions (*Magnezial'nye bazity…*, 1984; Likhachev, 1997). It seems to be the uncertainty in this issue that causes the wide spectrum of viewpoints concerning the differentiation mechanisms that predetermined the degree and direction of the magmatic evolution during its pre-chamber and in-chamber stages (see reviews of the problems of flood-basalt magmatism in the Siberian Platform: Sharma, 1997; Ryabov *et al.*, 2000).

The fact that the weighted mean composition of the Noril'sk-type intrusions is notably more magnesian than that of the typical "common flood basalt" (Table 1) led to the conclusion that a picritic basalt parental magma existed and was derived from a deep-seated source (Godlevskii, 1959). These concepts were further developed by researchers who assumed that the flood-basalt parental magma has a composition intermediate between typical picrite and flood basalt (*Magnezial'nye*

Table 1. Petrochemical characteristics of intrusive flood basalts in the Siberian Platform

Component	Differentiated intrusions				Average composition of flood-basalt magma	
	Noril'sk-1		Verkhne-Talnakhskii (Talnakh)		"normal" flood basalt	"average" flood basalt
	weighted mean (n = 54)	near-contact GD (n = 10)	weighted mean (n = 156)	near-contact GD (n = 2)		
	1	2	3	4	5	6
SiO_2	46.19	48.37	46.64	47.29	49.11	49.43
TiO_2	0.74	1.06	1.01	1.67	1.56	1.51
Al_2O_3	15.53	15.56	14.89	14.95	15.62	15.67
FeO	13.44	13.03	12.92	13.73	13.49	12.88
MnO	0.15	0.15	0.19	0.21	0.24	0.19
MgO	11.36	8.78	11.04	7.50	6.55	6.31
CaO	10.33	10.07	10.08	11.52	10.04	10.91
Na_2O	1.32	1.91	1.94	2.11	1.98	2.22
K_2O	0.69	0.92	1.11	0.89	0.85	0.75
P_2O_5	0.25	0.14	0.18	0.12	0.19	0.13

Note: References: (1) Godlevskii, 1959; (2–4) Dodin and Batuev, 1971; (5) Masaitis, 1958; (6) Kutolin, 1972. All Fe is given as FeO; analyses are normalized to 100%; GD is gabbro-dolerite.

bazity…, 1984). It was also assumed that this magma was primary, i.e., was derived by the melting of a mantle source at relatively high pressures and temperatures. Analysis of the fractionation schemes of such melts demonstrates a principal possibility of the origin of known "intrusive flood-basalt types" from a single source, which contained 10–12 wt % MgO and had a composition close to the weighted mean composition of the Noril'sk I intrusion (Table 1; Zolotukhin and Laguta, 1985; Zolotukhin and Vasil'ev, 1986). This implies an important role of the processes of pre-chamber differentiation, which may have occurred in magmatic columns or intermediate chambers (Likhachev, 1978; Oleinikov, 1979), mainly via the gravitational separation of crystals and melt. The modern interpretation of these processes is based on finer isotopic and geochemical differences (such as Mg#–TiO_2, REE patterns, Th/Ta ratios, etc.) between flood-basalt magmas, which can be interpreted as indications of the composition of the mantle source, the depth (pressure) and grade of its partial melting, and the extent of crustal contamination of magma (Naldrett *et al.*, 1992; Arndt *et al.*, 1993; Lightfoot *et al.*, 1993; Hawkesworth *et al.*, 1995). However, regardless of the picritic or picrite-like composition of the parental magmas, the concept of the deep-seated evolution of magnesian melts implies that these processes are responsible for the main differences between flood-basalt magmas, and the rocks crystallizing from them (including those of differentiated intrusions) inherit petrochemical and geochemical indications of these diversity.

At the same time, it is sometimes thought that the average compositions of solid flood basalts correspond to the partial melts of basaltic composition, whose source may have been mantle pyroxenites (Kutolin, 1972). Within the guidelines of this hypothesis, the insignificant fractionation of the parental flood-basalt magma, or the absence of fractionation, in deep-seated chambers are postulated, and the diversity of intrusive rocks is considered as resultant from contamination and in-chamber differentiation (Feoktistov, 1978). Hence, the problems of the Mg# of the parental magmas and the role of their differentiation at depth lies at the heart of discussions about the genesis and ore potential of ultramafic–mafic intrusions in the Siberian Platform. We believe that these problems can be resolved by determining the thermodynamic and dynamic parameters of magma intrusions for each individual intrusive body. The list of parameters should include the temperature and composition of the parental melt, its crystallization degree during intrusion, and the proportion and composition of mineral phases suspended in the melt. The amassment of such data would enable one to more reliably trace the possible genetic relations between the magmas of discrete flood-basalt intrusions and to gain better insight into the spatial distribution of the initial temperature, compositional, and phase parameters.

Such problems were first attacked by the computer simulation of the inner structures of flood-basalt intrusions in the Siberian Platform on the basis of the convection–cumulation mechanism of in-chamber differentiation (Frenkel' *et al.*, 1985, 1988). The examples of the Kuz'movka (on the Podkamennaya Tunguska

River), V-304, and Vavukan (in the upper reaches of the Vilyui River) sills were utilized to demonstrate that the parental magma contained no more than 8 vol % intratelluric crystals during its intrusion, with the solid phase consisting of excess *Ol* or the *Ol* + *Pl* assemblage. The application of these approaches to the Talnakh intrusion made it possible to explain the principal features of its inner structure as resultant from the chamber replenishment by a magma batch with a higher proportion of crystals: 15–20% intratelluric phases with olivine and plagioclase simultaneously present at the liquidus (Dneprovskaya *et al.*, 1987). Further developing this approach, we present the first estimates of the intrusion parameters of the Talnakh magma, which were obtained by the solution of the inverse geochemical problem by the computer simulation of melt–crystal equilibria in basaltic systems (Ariskin and Barmina, 2000).

GEOCHEMICAL THERMOMETRY TECHNIQUE

As follows from the materials published in the literature, the only method previously utilized to evaluate the composition of parental flood-basalt magmas was the calculation of the weighted mean compositions of the respective intrusions. Data of these type are fairly extensive and were used in distinguishing the association types of intrusions and developing schemes for their petrochemical classification (Vilenskii and Oleinikov, 1970). However, this approach fails to resolve several problems, in particular, as to why the composition of chill zones does not correspond to the average composition of the respective intrusions. This is clearly illustrated by the examples of the Noril'sk I and Talnakh intrusions: the average compositions of both massifs are significantly more magnesian than the compositions of the inner-contact gabbro-dolerites (Table 1). The main cause of these inconsistencies is the fact that the weighted mean composition of an intrusion can be accurately calculated only if full information of the volumetric percentages of all rock varieties is available. No correct assessment can be obtained on the basis of average chemical compositions or data on a few vertical sections (even if they are thoroughly studied), because this technique yields compatible estimates only for nearly ideal sheet-shaped bodies.

At the same time, the employment of inner-contact rocks as modeling the parental melt is also problematic because of their possible changes during interaction with the wall rocks. Furthermore, one of the most important criteria of their distinguishing, their fine-grained or subaphyric texture, can also be questioned (see, for example, Hoover, 1989). This criterion implies that the magma was homogeneous overheated melt. Several lines of evidence obtained over recent years indicate that melts injected in magma chambers contain variable amounts of crystalline phases (Frenkel' *et al.*, 1988; Mursh, 1989; Chalokwu *et al.*, 1993; Naslund and McBirney, 1996). This provides basis for another approach to the problem of intrusive magma and allows for different reconstructions of the parental melt compositions and the mechanisms of their in-chamber differentiation (Ariskin, 1999). The technique of geochemical thermometry was developed in the 1980s as means of assessment of the initial parameters of state on the basis of information "recorded" in the whole-rock compositions of volcanic and intrusive mafic rocks (Frenkel' *et al.*, 1987). This approach provides full phase and chemical interpretation of igneous rocks, including estimates of the original temperatures and composition of entrapped (intercumulus) melts (Barmina *et al.*, 1988). In certain cases, geochemical geothermometry makes it also possible to assay the phase composition of the intruded magma and the original composition of the intratelluric crystalline phases (Barmina *et al.*, 1989; Chalokwu *et al.*, 1993). We applied these approaches to the taxitic and picritic gabbro-dolerites of the Talnakh intrusion, whose inner structure is relatively simple and which shows typical features of differentiated ultramafic–mafic massifs of the Noril'sk type. As was noted by earlier researchers, the taxitic and picritic units should have played a determining role in the genesis of the sulfide mineralization (*Petrologiya i perspektivy rudonosnosti…*, 1978). Let us now consider some fundamental terms and physicochemical principles important for the analysis of geochemical thermometric data (Frenkel' *et al.*, 1987: Ariskin and Barmina, 2000).

Specification of the Petrological Terminology

In order to unambiguously interpret the results presented below, let us first specify the terms of magma and magmatic melt. One can find a diversity of definitions for them, with emphasis put on the aggregate state and rock-forming role of magmas in geological processes. For example, Kuznetsov (1990) stressed that magmas are, perhaps, physically homogeneous (silicate melt ± dissolved volatile components) or, more often, heterogeneous (melt + crystals) systems, "whose distinctive feature is fluidity, a property manifesting itself at >25% liquid in the mixture." Current discussions of the aggregate state of magmas are focused on the permitted proportions of crystals and melt, which characterize the unequal distribution of crystalline material from the full solidification boundary (walls of a magma conduit or chamber) inward the reservoir. The analysis of this situation leads to the recognition of two principal areas (Sinton *et al.*, 1992; Jaupart and Tait, 1995). A zone developing near the solidus surface has a low concentration of melt, which fills in the space between crystals. Touching by their edges and faces, the latter compose a rigid continuous framework, the so-called rigidus. In accordance with some of its rheological properties, this mixture behaves similarly to a solid but does not lose its plasticity. With a decrease in the percentage of crystalline material, the rigidus zone grades into crystalline mush and, further, to magmatic

suspension with <25% solid phases (Marsh, 1989). The rheological boundary between rigidus and mush is thought to correspond to a sharp (by a few dozen orders of magnitude) change in the dynamic viscosity at a concentration of crystalline material of roughly 50–60 vol % (Bergantz, 1990; Sharapov *et al.*, 1997). This value is referred to as critical crystallinity. The amounts of the complementary residual liquid define the critical melt fraction (see, for example, Renner *et al.*, 2000).

Hence, we will use the term *magma* to mean heterogeneous silicate systems with a concentration of individual crystals and/or their aggregates below the critical crystallinity. The liquid constituent of magma is magmatic melt. When overheated (i.e., contains no suspended solid phases), magma consists only of silicate liquid. In compliance with these definitions, the bulk chemical composition of any magma can be expressed through the compositions and proportions of suspended solid phases ($1 \le j \le M$) and melt (l)

$$C_i^{\text{mag}} = F_l C_i^l + \sum_{j=1}^{M} F_j^{\text{sus}} \overline{C}_i^j, \quad (1)$$

where i is a major or trace component, C_i^l is the magmatic melt composition, $\overline{C}_i^j$ is the weighted mean composition of crystals of a given mineral, and F_j^{sus} and F_l are the proportions of crystals and melts.

Not only magma as a whole but also magmatic melts, the principal constituents of magma, can be regarded as rock-forming systems, even if magmas are highly crystalline. We would like to stress this point because of the recent tendency to apply the term *magmatic melt* to compositions derived from the study of microscopic fragments of vitreous mesostasis or melt inclusions in minerals. In the latter instance, it seems to be reasonable to use, following A.V. Sobolev's proposal, the term *differential melts*, intended to highlight the bulk-composition heterogeneity of the final melt, a feature detectable when magmatic inclusions are examined in individual crystals (Sobolev, 1997). Natural melts, which serve as a transport medium, deliver to the surface some crystalline products of fractionation, and crystallize to magmatic rocks, were suggested to be termed *integral melts.* They are thought to be produced by the mixing of differential liquids during the prechamber stage. Within the framework of this terminology, we will focus on integral magmatic melts.

Parameters of the Genesis of Igneous Rocks

Early during its in-chamber differentiation, a magmatic system is mechanical mixture of crystals of different minerals ($1 \le j \le M$) and melt (l)

$$\sum_{j=1}^{M} F_j^{\text{cum}} + F_l^{\text{int}} = 1, \quad (2)$$

where F_j^{cum} and F_l^{int} are the initial proportions of mineral grains and silicate liquid. An apparent example of such a system is offered by cumulates, in which the relative movements of solid phases and melt are terminated by the development of a framework of cumulus grains. Relation (2) is also applicable to near-contact rocks, which cool rapidly and, because of this, can preserve the phase composition of the intruded magma or retain certain amounts of precipitating crystals. This initial state of the magmatic system can be defined as *the moment of the onset of rock development* in the geochemical sense, i.e., when the whole-rock composition is determined, which does not change if the system remains closed during its further cooling and recrystallization.

The bulk composition of a system of this type can be calculated from the relative proportions of its solid phases and melt, composition of the liquid phase $C_i^{l(0)}$, and the weighted mean concentration of a major or trace element in phenocrysts or cumulative grains of a given mineral species $\overline{C}_i^{j(0)}$

$$C_i^{\text{rock}} = F_l^{\text{int}} C_i^{l(0)} + \sum_{j=1}^{M} F_j^{\text{cum}} \overline{C}_i^{j(0)}. \quad (3)$$

The parameters of this equation provide the full description of the initial state of magmatic mixture, whose solidification gave rise to rocks. This makes it possible to determine the values of F_j^{cum} and F_l^{int} as *the original phase proportions* and $\overline{C}_i^{j(0)}$ and $C_i^{l(0)}$ as *the initial compositions of crystals and melt.* The original melt is characterized by a certain liquidus temperature, which can be referred to as *the temperature of rock origin.* This definition applies only to the initial condition of the existence of a melt–mineral assemblage, and normally it is simply the temperature of liquid entrapped in the intercumulus. Hence, it is in the bulk composition of a rock that contains the "record" of the initial state, and the reconstruction of the conditions of rock genesis can be formulated as the utilization of this information for assaying the initial phase proportions and compositions.

Justification of Geochemical Thermometry

One of the basic assumptions is as follows: during the initial moment of the origin of rocks of a massif, the compositions of minerals and melt, $C_i^{l(0)}$ and $\overline{C}_i^{j(0)}$, are related by the equations of thermodynamic equilibrium, which involve, as one of their parameters, the temperature of rock origin. This temperature corresponds to the initial conditions of the existence of the melt–crystal assemblage and affects, as an equilibrium factor, the distributions of major and trace elements

between the phases. Another fundamental assumption is that the whole diversity of rocks in an examined massif can provide samples whose chemical variations were caused only by changes in the initial phase proportions, F_j^{cum} and F_l^{int}. These samples represent rock groups that were produced by melt at the same temperature and minerals of the same composition.

An important feature of these rocks is that their equilibrium melting may yield series of melts that are characterized by distinct evolutionary trajectories in temperature–composition plots, but their melting curves inevitably have points that correspond to a temperature at which the compositions of all liquids are identical, i.e., these lines should intersect either at a point or within a compact area. It is easy to realize that this composition should correspond to the composition of the entrapped liquid (the same for all rocks), and the deduced temperature is the formation temperature of these rocks. This statement can be proved by contradiction: if no such an intersection occurs, this would mean that no mass balance condition holds for the chosen rock compositions or the initial compositions of minerals, $\bar{C}_i^{j(0)}$, and melt, $C_i^{l(0)}$, are not related by thermodynamic equilibrium laws. Thus, to determine the initial formation parameters of a given intrusive rock, one should: (1) select a few additional samples whose entrapped melt composition is supposedly similar; (2) conduct a physical experiment on or numerical simulation of the equilibrium melting of this group of rocks; (3) determine or compute the compositions of the resultant melts; and (4) construct the evolutionary trends for the model liquids in a temperature–composition plot and determine the point (or area) of their intersection.

Application of the Method

In application to intrusive mafic rocks, the constancy of the entrapped or residual magmatic liquid allows for two variants of their genetic and geological interpretation. First, this may have resulted from the local (on a scale of a few centimeters to a few meters or, at most, dozens of meters for large layered complexes) heterogeneity of the rocks and, as the limiting case, microscopic-scale cyclic layering. Second, this could have been caused by the weak fractionation of the magma, which implies the existence of similar formation conditions for rocks throughout a given geologic body. Ideally, it is most desirable to have a few groups of genetically interrelated rocks distributed over the vertical section of the intrusion or throughout its volume. This would make it possible to refine the character of melt evolution during the in-chamber differentiation and the possible compositional heterogeneity of the magmatic liquid in different parts of the intrusion.

From the viewpoint of estimating the composition of the original (during its intrusion) magmatic melt, the most informative data can be provided by inner-contact and near-contact rocks, for which it is quite realistic to suggest the compositional homogeneity of the entrapped liquid. An illustrative example of the efficiency of this approach give the results of geochemical thermometry on the near-contact *Ol–Pl* cumulates of the Skaergaard intrusion, which were sampled within 10 m from the contact and are referred to as the Side Marginal Group (Ariskin, 1999). It is hard to assay the possibility that an analogous research can be conducted on the rocks of the Talnakh intrusion, because this requires systematic information on the chemistry of the inner-contact gabbro-dolerites of as much as possible contrasting compositions. At the same time, numerous analyses of the taxitic and picritic gabbro-dolerites from the lower parts of the massif are available from the literature.

Provided the Talnakh magma was not overheated and entrained a certain amounts of intratelluric olivine (and, possibly, also plagioclase) into the chamber, the compositional variations of rocks from the lower part of the massif can be regarded as resulting from the redistribution and sorting of crystals without significant fractionation of silicates in the main volume of the magmatic melt (Dneprovskaya *et al.*, 1987). When used in this case, the geochemical thermometry method allows one to constrain the formation parameters of the taxitic and picritic gabbro-dolerites, whose temperature, mineral chemistry, and melt composition should be similar to those of the parental intrusive magma. The correctness of the aforesaid assumption and the estimates obtained may be tested by the consistency of the calculated and observed compositions of the rock-forming minerals.

The approach proposed above can be realized with the COMAGMAT-3.5 computer program (Ariskin, 1999; Ariskin and Barmina, 1999). The program was developed for simulating the crystallization of basalts of low and moderate alkalinity within predetermined ranges of pressure and oxygen fugacity. The possibility of its application to geochemical thermometry is justified by the fact that equilibrium crystallization and melting processes are reversible, and the calculation of a melting trajectory can be replaced by the calculation of equilibrium crystallization of the respective melt. When a relatively small number of compositions is involved, the intersections points of the calculated evolutionary paths can be found by the visual analysis of a series of *T–X* diagrams. Therein it should be taken into account that the analytical errors and uncertainties involved into the phase equilibrium model cause certain errors in the determined intersection of the calculated crystallization trajectories and, hence, this intersection occurs in a *T–X* plot as an area with closely spaced evolutionary lines (see below). In working with the COMAGMAT program on tholeiite-like systems, the errors of temperature estimates are of the orders of the employed thermometers, i.e., 10–15°C, with the major-component concentrations calculated accurate to 0.5–1 wt % (Ariskin and Barmina, 2000).

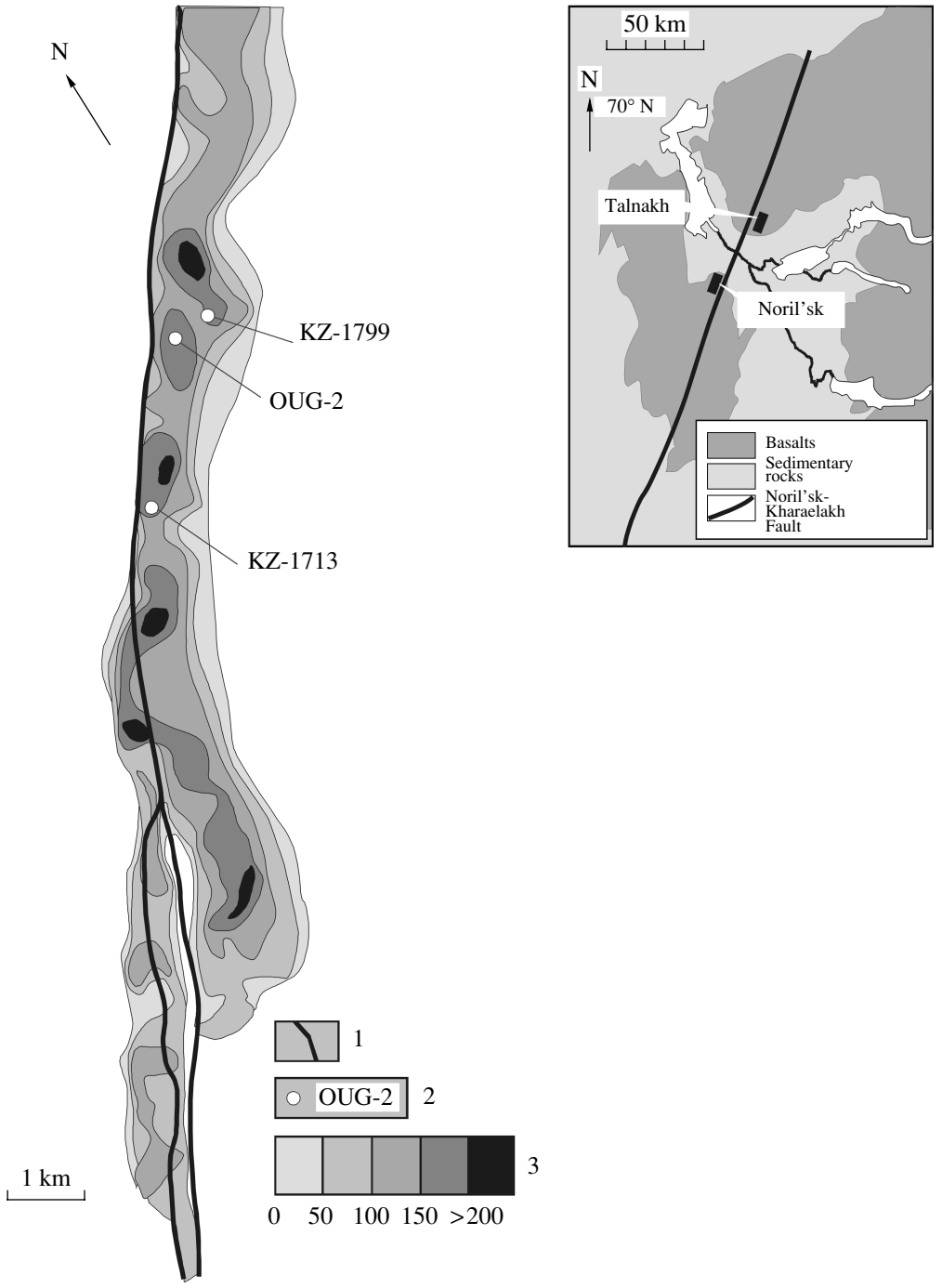

Fig. 1. Schematic map showing the setting of the Talnakh intrusion in the Noril'sk district and the morphology of the intrusion (projection onto a horizontal plane).
(1) Faults; (2) holes and their numbers; (3) gradation of the intrusion thickness, m.

DISTINCTIVE STRUCTURAL AND COMPOSITIONAL FEATURES OF THE TALNAKH INTRUSION

The geology and tectonic setting of the Talnakh Massif are controlled by the Noril'sk–Kharaelakh deep fault, which is the Main Tectonic Suture with subparallel systems of westerly and easterly normal faults and associated plication structures. Morphologically, this intrusion is a chonolith with a flat or, in places, smoothly convex roof and a smoothly concave floor (Fig. 1). The massif is traced for 20 km and has a width of 0.5–2 km at a maximum thickness of 218 m. The body dips 4–6° NNE and, hence, its roof occurs in contact with the Permian Ergalakh Formation in the south

and the Lower Devonian Zubovskaya Formation in the north. The geology and inner structure of the Talnakh intrusion were described in much detail in several earlier publications (Dodin and Batuev, 1971; Zolotukhin *et al.*, 1975; Distler *et al.*, 1988; Dyuzhikov *et al.*, 1988; Likhachev, 1994; Zen'ko and Czamanske, 1994; Czamanske *et al.*, 1995; Ryabov *et al.*, 2000).

Inner Structure and Petrography

Similarly to other massifs of the Noril'sk type, the Talnakh intrusion is characterized by a layered inner structure with systematically alternating rocks in a vertical section. The succession of derivatives is normally visualized as a layered series with the following three units (listed in order from bottom to top): the *Lower Gabbro Series* (contact and taxitic gabbro-dolerites), the *Main Layered Series* (picritic, olivine–biotite, olivine, olivine-bearing, and olivine-free gabbro-dolerites), and the *Upper Gabbro Series* (gabbro-diorites, ferrogabbro, upper-contact gabbro-dolerites, eruption breccias, upper picritic gabbro-dolerites, leucogabbro, and taxitic chromite-bearing gabbro). All units are typically present in the central part of the intrusion, and its peripheral parts are devoid of picritic gabbro-dolerites, and, consequently, the inner structures of these parts are more homogeneous.

The lowermost one-third of the massif (the Lower Gabbro Series and the bottom of the Main Layered Series) is the most compositionally contrasting and contains, in addition to a horizon of olivine-rich (up to 50–60 vol % *Ol*) rocks, leucogabbro, whose plagioclase concentration may reach as high as 70 vol %. The latter rocks are characterized by a very heterogeneous texture and are referred to as taxitic gabbro-dolerites or taxites in the Russian literature. We attract attention to this fact and highlight the strong heterogeneity of the lower part of the intrusion because the most reliable results are yielded by geochemical thermometric techniques for rocks of contrasting mineralogical and chemical composition (Ariskin and Barmina, 2000).

The Main Layered Series is characterized by gradual transitions between its rocks, mainly due to the systematic upward decrease in the *Ol* concentration. The most typical rocks of the Upper Gabbro Series are gabbro-diorites, ferrogabbro, and near-contact gabbro-dolerites, all of which are variably altered. The leucocratic gabbro do not form an individual layer but occur as lenses of different thicknesses (up to 25 m) and lengths (from a few to a few hundred meters). The *Ol*-rich rocks (picrite- and troctolite-like) are rare in the upper contact zone of the massif and normally develop in the form of relatively thin (no more than 0.5 m) lenses in the upper parts of the leucogabbro.

The inner structure, mineralogy, and chemistry of the Talnakh intrusion are described below based on the data recovered by reference Hole OUG-2, which was drilled in the central part of the massif (Fig. 1). The penetrated intrusive rocks attain 155 m in thickness. From its bottom to top, the magmatic succession consists of (A) lower near-contact and taxitic gabbro-dolerites, (B) picritic gabbro-dolerites, (C) olivine gabbro-dolerites, (D) olivine-bearing gabbro-dolerites, (E) olivine-free gabbro-dolerites, (F) gabbro-diorites and prismatic-granular gabbro-dolerites, (G) leucocratic, sometimes taxitic gabbro, and (H) upper-contact gabbro-dolerites, quartz diorites, and eruption breccias (Fig. 2).

A. *Near-contact gabbro-dolerites* (1.5–2 m) compose the lower and upper marginal zones. These are fine- and small-grained rocks with microdoleritic, ophitic, or poikilophitic textures of the groundmass, which sometimes contains plagioclase (An_{70}) phenocrysts. The average composition of the rocks is as follows: 50–60 vol % *Pl*, 32–40% *Cpx*, 5–10% *Ol*, and 5–15% ore minerals, the subordinate minerals are hornblende, biotite, apatite, and sphene. Olivine (Fo_{64}) and ore minerals occur only in the lower-contact gabbro-dolerites.

Taxitic gabbro-dolerites (13 m), are light gray and white coarse-grained rocks with a clearly pronounced ataxitic structure, which is caused by the contrasting grain sizes and uneven distribution of mafic minerals. The mineralogical composition of the rocks varies within wide limits: 35–75% *Pl* (of two generations, $An_{51–66}$ and $An_{76–83}$), 10–30% high-Ca *Cpx* ($Fs_{10–12}$), 5–25% *Ol* ($Fo_{62–82}$), and up to 5% *Opx* ($Fs_{21–25}$). The rocks are characterized by variable structures and textures, with variations often observable even within a single thin section.

The dominant textural pattern is determined by large (3–5 mm) zoned tabular plagioclase grains ($An_{66–57}$ and $An_{83–76}$), whose marginal parts are more sodic, up to An_{30}, with inclusions of anhedral clinopyroxene grains. The clinopyroxene (up to 5 mm) contains inclusions of small (<1 mm) tabular crystals and laths of plagioclase and grains of olivine and thus causes the poikilophitic texture of the rock. The clinopyroxene is often zoned, with green inner and brownish outer zones.

Along with these coarse-grained patches, the rocks contain finer grained zones (with grains <1 mm) consisting of *Pl* laths (with occasional *Cpx* grains in between) and having a clear ophitic texture. These rocks sometimes have a gabbro texture, which is caused by roughly equally euhedral equant *Pl* and *Cpx* grains. The taxites also bear relatively small (up to 1–2 cm) lens-shaped segregations of fine-grained (0.1–0.3 mm) *Ol* and *Pl* (sometimes with an admixture of Al–Mg spinel), whose composition corresponds to troctolite. Olivine most often develops in these rocks as anhedral grains with inclusions of tabular plagioclase crystals.

Oxides account for up to 5 vol % of the rocks. These are titanomagnetite and ilmenite. The taxitic gabbro-dolerites compose (along with picritic gabbro-dolerites) a mineralized unit, whose sulfide concentration attains 10–15 vol %. The ore minerals generally occur

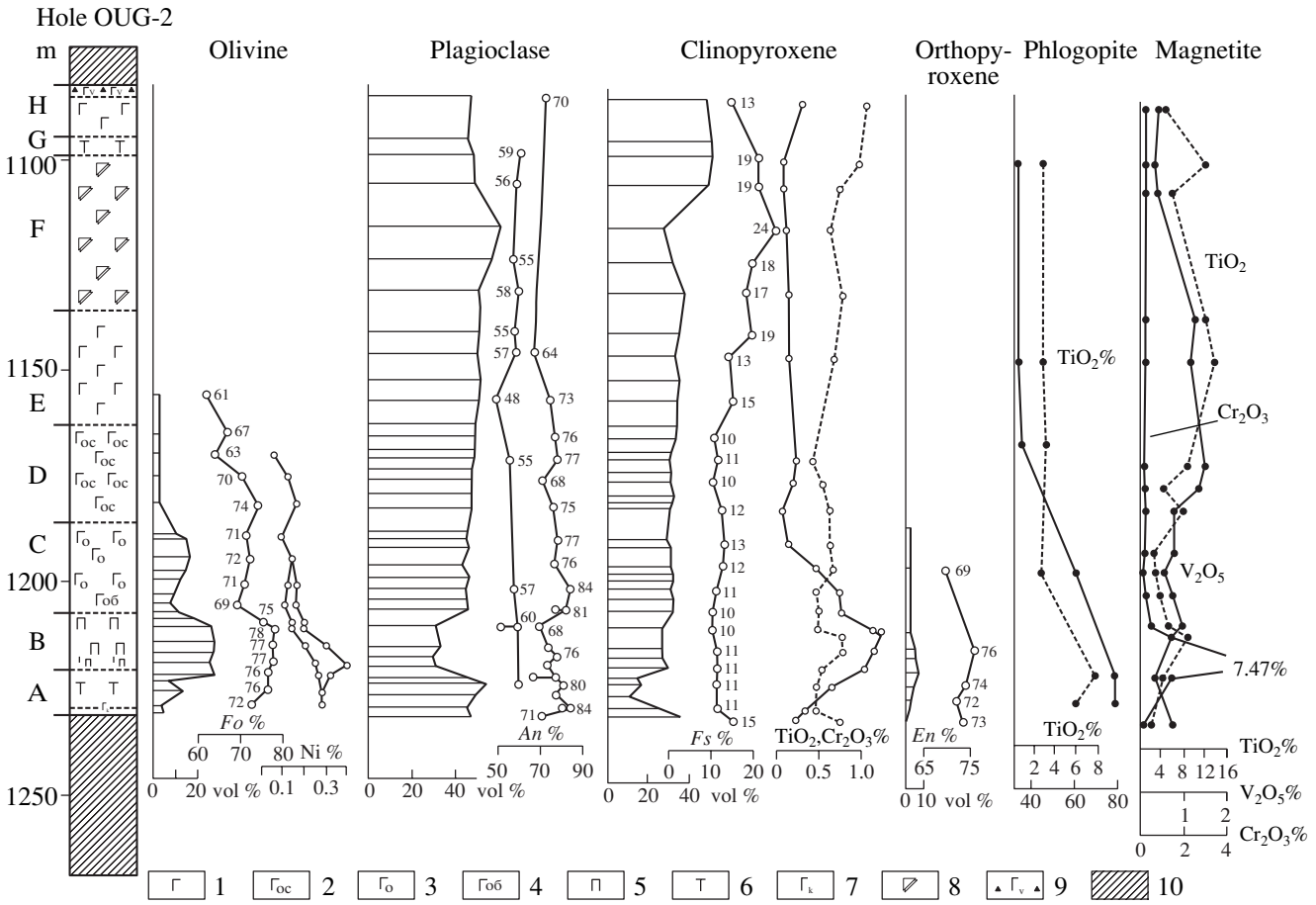

Fig. 2. Variations in the concentrations and composition of rock-forming minerals in the vertical section of the Talnakh intrusion (Hole OUG-2).

Here and in Figs. 3 and 7: (1–7) gabbro-dolerite (1—olivine-free, 2—olivine-bearing, 3—olivine, 4—olivine–biotite, 5—picritic, 6—taxitic, 7—near-contact); (8) gabbro-diorite; (9) eruption breccia; (10) vein-disseminated, and massive ores.

as large (up to 5 cm) anhedral pockets and schlieren. The secondary alterations of the taxites involve saussuritization of plagioclase, clinopyroxene replacement by hornblende, and biotite replacement by chlorite. The rocks usually smoothly grade into the overlying picrites.

B. *Picritic gabbro-dolerites* (14 m) compose a unit with clear-cut lower and, particularly, upper boundaries. It consists of dark gray fine- to medium-grained massive rocks, in which *Ol* accounts for less than 25 vol % (sometimes up to 70%). The picrites mostly have poikilophitic, poikilitic, and, in places, panidiomorphic-granular textures. The average mineralogical composition of the rocks is as follows: 25–30% *Ol* ($Fo_{72–78}$), 30–35% *Pl* ($An_{53–66}$ and $An_{72–84}$), 30–35% augite ($Fs_{10–11}$), up to 5% *Opx* ($Fs_{20–23}$), and 5–7% *Bt*. The accessory minerals are apatite and sphene.

The olivine is distributes relatively equally over the rock and occurs as euhedral grains 0.3–1 mm in size, without notable zoning. The plagioclase develops in the form of large (up to 1.5 mm) tabular crystals (with included euhedral olivine crystals) and anhedral grains with pronounced zoning. Another plagioclase generation, laths included in clinopyroxene, has clear twins.

The clinopyroxene (augite) occurs as oikocrysts from 1–3 to 5 mm with inclusions of *Ol* grains and *Pl* platelets. The orthopyroxene is present in strongly subordinate amounts, as euhedral prisms or, more rarely, oikocrysts with *Ol* inclusions. *Opx* sometimes develops as thin rims around *Ol*. Brown biotite forms lepidoblastic aggregates, which often tend to develop near oxide and sulfide inclusions and replace clinopyroxene. The latter, in turn, is also replaced by hornblende. The olivine is typically replaced by minerals of the serpentine group (with replacement grades varying even within a single thin section), first along fractures (together with magnetite and pyrrhotite) and, later, in the form of aggregates of lizardite platelets.

The oxides (titanomagnetite, ilmenite, Cr-magnetite, and chromite) account for 3–5% by volume, with the contents of sulfides attaining 5–8%. The latter minerals are present as fine-grained (<2 mm) interstitial dissemination in the upper portion of the picrite layer and predominantly as ovoids up to 25 mm across in the

middle and lower parts of the unit. The transition zone to taxitic gabbro-dolerites contains segregations of large plagioclase grains, whose concentration increases downward, with these segregations eventually merging and the rock acquiring a typical taxitic fabric.

C. The transition to the overlying *olivine gabbro-dolerites* (20 m) is relatively sharp and occurs within a 0.1- to 0.3-m zone. The olivine gabbro-dolerites are gray, medium-grained, massive rocks, which are characterized by poikilophitic and ophitic textures. Their *Ol* ($Fo_{69–75}$) concentration attains 10–15 vol %, *Pl* ($An_{57–60}$ and $An_{75–84}$) accounts for 40–50 vol %, and *Cpx* ($Fs_{11–13}$) and *Opx* (Fs_{26}) are present in amounts of 25–30 and up to 3%, respectively. The boundary between these rocks and picrites is marked by elevated contents of biotite (up to 6–7%) and sulfides. The accessory minerals are apatite and sphene, the secondary minerals are prehnite, carbonates, iddingsite, chlorite, and serpentine).

D and E. *Olivine-bearing and olivine-free gabbro-dolerites* (60 m) gradually replace the underlying unit due to a gradual systematic upsection decrease in the content of *Ol* up to its full disappearance and the replacement of the gabbrophitic, poikilophitic, and panidiomorphic-granular textures by prismatic-ophitic and prismatic-granular textures. The main rock-forming minerals are *Pl* ($An_{55–57}$ and $An_{64–77}$), *Cpx* ($Fs_{10–19}$), *Ol* ($Fo_{61–71}$), and *Opx*. The rocks sometimes contain quartz in the upper part of the unit. The rocks also often contain oxides and disseminated sulfides. The accessory and secondary minerals are the same as in the rocks of the underlying units.

F. *Gabbro-diorites and prismatic-granular gabbro-dolerites* (30 m) are medium- to coarse-grained greenish or pinkish gray rocks with prismatic-granular, ophitic textures, containing schlieren of pegmatoid gabbro-dolerites and thin layers of titanomagnetite gabbro. The rocks consist of 50–70 vol % *Pl* ($An_{56–59}$) and 20–30% augite ($Fs_{17–24}$). The mesostasis contains albite, microcline, quartz, biotite, chlorite, pumpellyite, orthite, apatite, zircon, and sphene. The secondary minerals are aegirine-augite, hornblende, chlorite, saponite, hydrotalcite, prehnite, and saussurite aggregates.

G. *Taxitic gabbro* (4 m) in the upper portion of the massif are very unequally grained leucogabbro of ataxitic structure and consist of 60–70% *Pl* ($An_{60–70}$), 20–25% *Cpx* (Fs_{20}), hornblende, biotite, rare grains of quartz, micropegmatite, sphene, apatite, and carbonates. In places, the rocks of this unit acquire unchanging textures and structures and become common anorthite leucogabbro. The taxitic gabbro often host low-sulfide platinum mineralization. These rocks are enriched in chromite and contains aggregates of H_2O-, Cl-, and F-bearing minerals (Sluzhenikin *et al.*, 1994).

H. *Quartz diorites* (13 m) compose the roof of the intrusion. These are compositionally, texturally, and structurally variable rocks, which include clearly bounded shadow xenoliths of the host sand–siltstones of the Tungusska Group. The rocks consist of quartz, potassic feldspar, sodic plagioclase, micropegmatite, biotite, hornblende, relict clinopyroxene, apatite, and fragments of microquartzite, hornfelsed carbonaceous rocks, and graphitized coal, which compose the eruption breccias.

Cryptic Layering of the Talnakh Intrusion

The compositional trends of the principal rock-forming minerals over the section of Hole OUG-2 are demonstrated in Fig. 2. Tables 2 and 3 list representative analyses of olivine, plagioclase, and clinopyroxene, which were used in distinguishing units.

Olivine. The compositional changes of this mineral in distinct zones of the massif are particularly significant. The maximum forsterite concentration ($Fo_{82.3}$) was detected in the upper part of the taxitic unit (Fig. 2, Table 3), although the overlying picritic gabbro-dolerites usually have more magnesian compositions. In the olivine gabbro-dolerites, *Fo* varies from 69 to 72 mol %, and the Mg# of *Ol* decreases to $Fo_{61.3}$ with the transition to *Ol*-bearing gabbro-dolerites. These variations are correlated with the NiO concentration of *Ol*, which ranges from 0.20–0.25 wt % in the picrites to 0.08–0.11 wt % in the *Ol*-bearing gabbro-dolerites. The MnO and CaO concentrations of olivine simultaneously increase upsection.

Plagioclase. Two generations of this mineral can be distinguished: (1) large platelets of zoned plagioclase, whose composition varies from $An_{75–84}$ in the olivine, picritic, and taxitic gabbro-dolerites and the upper anorthite leucogabbro to $An_{56–39}$ in the gabbro-diorites; and (2) intercumulus plagioclase with polysynthetic and simple twins and less pronounced compositional variations, roughly from An_{62} to An_{47} (Fig. 2). Both generations exhibit a common tendency: plagioclase becomes more sodic upsection, up to the development of albite, which is widespread in the gabbro-diorites.

Clinopyroxene. The concentration of *Cpx* systematically increases from bottom to top from 15–25 vol % in the picrites to 40–45 vol % in the rocks of the Upper Gabbro Series. The mineral can be subdivided into two varieties: (1) green and (2) brown, with the predominance of *Cpx* of the first type. Both varieties correspond to augite, although green grains are more magnesian and chromic, and brown grains are more titanic (Dobretsov *et al.*, 1970; Zolotukhin *et al.*, 1975; Czamanske *et al.*, 1995). The compositions of clinopyroxene from the rocks of the Upper Gabbro Series fall within the field of typical augite (Hess *et al.*, 1941), and augite from the rocks of the Main Layered and Lower Gabbro series are more magnesian and close to the field of endiopside. A single clinopyroxene grain usually has a more Fe-rich rim than its core.

The composition of clinopyroxene systematically varies over the vertical section of the massif. The concentration of the ferrosilite end-member increases upward, from 10–11 mol % in the picrites and taxites to

Table 2. Chemical composition of rocks from the Talnakh intrusion (Hole OUG-2)

Component	1	2	3	4	5	6	7	8	9	10	11	12
	1104.6*	1130.3	1144.4	1169.2	1181.6	1188.3	1200	1208	1213.7	1218	1222.8	1230
SiO_2	46.43	47.21	49.66	49.01	46.79	46.57	46.69	40.49	37.66	38.96	41.49	43.34
TiO_2	2.3	1.47	1.15	0.89	0.71	0.83	0.72	0.6	0.4	0.44	0.55	0.54
Al_2O_3	12.38	13.45	14.51	15.99	17.32	16.78	17.32	8.02	7.9	7.75	11.22	14.01
Fe_2O_3	7.11	5.15	4.02	4.26	4.29	3.68	3.88	4.81	6.59	4.6	11.45	8.76
FeO	9.11	9.32	7.98	5.64	4.94	7.4	6.06	10.79	12.52	12.6	7.06	6.75
MnO	0.23	0.24	0.23	0.18	0.15	0.18	0.16	0.22	0.18	0.23	0.15	0.15
MgO	5.11	6.28	6.13	7.11	8.86	10.43	10.05	22.41	18.77	19.13	7.15	6.64
CaO	9.25	10.1	10.77	12.21	10.98	9.32	10.84	5.3	5.01	4.96	5.53	9.22
Na_2O	3.58	2.32	2.5	2.18	1.98	1.92	1.81	0.87	0.88	0.62	2.22	1.94
K_2O	0.99	0.83	0.67	0.69	0.49	0.57	0.46	0.25	0.32	0.41	1.09	0.79
Cr_2O_3	<0.007	<0.007	<0.007	0.053	0.071	0.02	0.089	0.77	0.57	0.28	0.033	0.034
P_2O_5	0.27	0.25	0.25	0.15	0.14	0.17	0.15	0.12	0.11	0.11	0.15	0.14
H_2O^-	0.14	0.43	0.24	0.2	0.38	0.26	0.2	0.14	0.22	0.78	0.22	0.24
H_2O^+	1.67	1.29	1.59	1.51	2.35	1.75	1.89	4.49	2.96	6.05	2.12	1.79
Ni	0.01	0.01	0.01	0.01	0.28	0.35	0.04	0.17	0.53	0.45	0.89	0.59
Co	0.01	0.01	0.01	0.01	0.01	0.01	0.01	0.02	0.03	0.02	0.04	0.03
Cu	0.01	0.02	0.02	0.01	0.01	0.01	0.01	0.13	1.58	0.30	3.00	1.79
S	0.33	0.2	0.25	0.091	0.076	0.13	0.051	0.45	4.23	2.33	7.24	4.85
CO_2	0.64	0	0	0	0	0	0	0	0	0	0	0
F	0.11	0.08	0.08	0.06	0.06	0.06	0.05	<0.05	<0.05	0.07	0.06	0.06
Total	99.68	98.66	100.06	100.25	99.88	100.44	100.48	100.04	100.47	100.09	101.66	101.66

Note: Analyses were conducted at the Central Chemical Laboratory of the Institute of the Geology of Ore Deposits, Petrography, Mineralogy, and Geochemistry, Russian Academy of Sciences, analysts E.P. Frolova and N.V. Koroleva. Rocks: (1–12) gabbro-dolerite (1–3 – prismatic-granular, 4 – *Ol*-free, 5 and 6 – *Ol*-bearing, 7 – olivine, 8–10 – picritic, 11 and 12 – taxitic).
* Depth, m.

24 mol % in the gabbro-diorites, and then decreases to 13 mol % in the upper marginal gabbro-dolerites. The concentration of the enstatite component accordingly decreases upward from 53 to 35 mol %, whereas the concentration of the wollastonite end-member simultaneously varies relatively little, from 38 to 44 mol %. The Cr_2O_3 concentration of the pyroxenes attains a maximum of 1.13–1.21 wt % in the uppermost one-third of the picrite unit and then rapidly decreases toward the taxitic gabbro-dolerites. The systematic decrease in the Cr_2O_3 content of *Cpx* is also characteristic of the transition from the picrites to olivine and olivine-bearing gabbro-dolerites. The behavior of TiO_2 is characterized by smaller variations, but its steady enrichment was detected in the upper inner-contact zone (Table 3), particularly, in the gabbro-diorites.

Orthopyroxene. The most magnesian orthopyroxene, with 76 mol % *En*, was encountered in the picritic gabbro-dolerites. Up and down the section, the Mg# of this mineral decreases, and its Fe# correspondingly increases (Fig. 2). The orthopyroxene from the picritic gabbro-dolerites is characterized by the highest concentrations of Cr_2O_3 (0.47 wt %), with other components varying as follows: Al_2O_3 from 0.7 to 1.15 wt %, CaO from 1.6 to 2.4 wt %, MnO from 0.35 to 0.50 wt %, and TiO_2 from 0.4 to 0.65 wt % (Table 3).

Biotite. The composition of biotite varies over a broad interval in the vertical section of the Talnakh Massif (Fig. 2, Table 3). The biotite of the olivine, picritic, and taxitic gabbro-dolerites is the highest in MgO (15–18 wt %), TiO_2 (6–7 wt %), and alkalis (8.4–9.1 wt %) at a minimum concentration of CaO. This mineral in the upper derivatives of this intrusion (upper taxites, leucogabbro, gabbro-diorites, and olivine-free and olivine-bearing gabbro-dolerites) has a relatively low Mg# and is low in alkalis but high in CaO (up to 0.5 wt %) at a TiO_2 concentration of 2.4–2.6 wt %.

Major- and Trace-Element Chemistry of the Rocks

The chemistry of typical rocks from the Talnakh Massif (samples recovered by Hole OUG-2) is illustrated by the data of Table 2, and the corresponding distribution of elements over the vertical section of the

Table 3. Chemical composition (wt %) of rock-forming minerals from the Talnakh intrusion (Hole OUG-2)

Depth, m	SiO_2	TiO_2	Al_2O_3	Cr_2O_3	FeO	MnO	MgO	CaO	Na_2O	K_2O	NiO	Total	Recalculated end-members
Olivine													*Fo*, mol %
1156.2 E	36.75	0.03	0.08	0.03	33.24	0.63	29.55	0.38	0	0.02	0.08	100.79	61.3
1164.5	37.03	0.02	0.06	0.01	28.60	0.61	33.39	0.29	0	0.01	0.05	100.07	67.5
1169.2	36.23	0.02	0	0.03	32.14	0.65	31.29	0.34	0	0.02	0.08	100.80	63.0
1175.0 D	38.16	0.03	0	0.04	26.00	0.54	34.80	0.30	0	0.01	0.11	99.99	70.0
1181.6	38.09	0.02	–	0.01	23.94	0.47	36.90	0.38	0.04	0.02	0.13	100.00	73.6
1188.3	37.28	0.02	0.08	0.01	25.48	0.46	35.15	0.30	0.03	–	0.08	98.90	70.9
	38.35	0.02	0.17	0.01	24.75	0.44	37.11	0.34	–	–	0.13	101.32	73.0
1200.0 C	37.67	0.03	0.09	0.04	25.10	0.45	35.75	0.36	–	–	0.13	99.62	71.6
	36.44	0.10	0.08	–	27.53	0.43	34.64	0.26	0.09	–	0.09	99.58	68.9
1208.0	37.20	–	0.12	–	23.78	0.44	37.70	0.31	0.07	–	0.13	99.75	74.2
1209.5 B	38.72	–	0.11	–	19.28	0.31	41.60	0.29	–	–	0.13	100.44	79.7
1218.0	38.37	0.03	0.06	0.03	21.83	0.36	40.12	0.10	0	0	0.25	101.76	76.7
	38.31	0.03	0.02	0.01	21.09	0.37	39.49	0.13	0	0	0.18	99.66	77.1
1221.2	39.31	0.05	0	0.07	17.04	0.31	43.27	0.15	0	0	0.22	100.43	78.5
	38.63	0.05	0	0.01	16.78	0.30	43.64	0.14	0	0	0.20	99.76	82.3
1221.8	37.82	0	0	0	21.97	0.32	39.74	0.20	0	0	0.18	100.24	76.4
1222.8 A	35.12	0.03	0.02	2.49	25.30	0.40	34.17	0.20	0	0	0.19	97.94	70.2
1225.7	37.90	0.02	0.02	0	24.20	0.41	38.12	0.17	0	0	0.19	101.10	74.0
	38.57	0.07	0	0	21.62	0.34	40.29	0.11	0	0	0.19	101.20	77.0
1227.5	38.95	0.02	0	0.03	24.45	0.50	36.69	0.14	0	0	0.19	101.11	72.4
	38.93	0.02	0	0.03	24.57	0.50	35.90	0.14	0	0	0.19	100.44	71.8
Plagioclase													*An*, mol %
1085.6 H	50.89	0.03	28.95	0.01	1.18	0	0.36	14.55	3.32	0.17	–	99.46	70.2
1097.9 G	52.56	0.17	27.10	0.03	1.21	0	0.32	11.98	4.39	0.24	–	98.00	59.3
	57.00	0.08	26.25	0	0.75	0	0.05	9.82	5.82	0.34	–	100.11	47.3
1104.6	55.29	0.05	26.59	0	0.76	0	0.10	10.70	4.37	0.29	–	98.15	56.5
1116.5	68.73	0	20.53	0.04	0.08	0	0	0.71	11.54	0.06	–	101.69	3.4
1123.5 F	54.99	0.07	27.01	0.01	0.93	0.01	0.10	11.55	5.08	0.22	0	99.97	55.2
1130.3	53.86	0.07	27.80	0.09	1.10	0.04	0.26	12.02	4.61	0.21	0	100.06	58.1
	53.19	0.05	28.42	0	0.82	0.01	0.12	12.44	4.77	0.16	0	99.98	58.6
1139.2	58.95	0.10	24.17	0.01	0.99	0.03	0.13	7.81	7.02	0.57	0	99.76	37.0
	53.09	0.03	27.59	0.01	0.95	0.01	0.08	11.63	4.83	0.27	0	98.51	56.5
1144.4 E	53.45	0.03	28.49	0.07	0.97	0.01	0.36	13.18	4.02	0.17	0	101.20	63.8
	56.0.8	0.05	27.05	0	0.76	0.01	0.07	9.90	5.78	0.30	0	100.00	57.4
1156.2	50.67	0.02	31.51	0	0.90	0.05	0.18	15.12	3.11	0.19	0	101.71	72.6
	56.23	0.20	26.76	0.01	1.51	0	0.13	9.89	5.65	0.40	0	100.83	48.2
1164.5	48.85	0.02	30.86	0.03	0.73	0.01	0.13	15.08	2.51	0.13	0	98.34	76.4
1169.2	48.88	0.03	31.36	0	0.93	0.04	0.33	15.71	2.52	0.10	0	99.87	77.1
D	54.39	0.07	28.24	0	0.79	0.04	0.08	10.34	4.53	0.30	0	98.78	54.6
1175.0	52.32	0.03	29.54	0.03	1.00	0.01	0.32	13.72	3.49	0.17	0	100.63	68.0
1181.6	49.54	–	31.71	–	0.75	–	0.22	16.12	2.83	0.11	–	101.58	75.3
1188.3	50.69	0.03	28.37	–	0.79	–	0.18	15.58	2.45	0.08	–	98.17	77.4
1194.4	50.37	–	29.60	–	0.75	–	0.22	16.26	3.01	0.13	–	100.34	74.5
1200.0 C	53.82	0.07	27.76	–	1.07	–	0.45	11.84	4.72	0.29	–	100.02	57.2
	47.94	–	32.16	–	0.74	–	0.12	17.18	1.78	0.06	–	99.98	83.9
1204.8	49.88	0.05	30.22	–	0.82	–	0.25	15.86	2.63	0.12	–	99.83	76.3
	48.51	0.03	31.32	–	0.98	–	0.40	16.06	2.04	0.11	–	99.45	81.0
1208.0	51.93	0.08	28.26	–	1.00	–	0.40	12.40	4.45	0.25	–	98.77	59.7
	53.41	0.07	27.54	0.01	1.48	0.01	0.40	10.67	5.03	0.18	–	98.80	53.2
1209.5 B	51.49	0.02	31.17	0.01	0.75	–	0.41	13.36	3.33	0.13	–	100.67	68.2
1218.0	50.05	0.05	30.86	0	0.72	0	0.05	14.27	3.03	0.16	0	99.22	71.7
1221.2	48.38	0.03	31.85	0	0.54	0	0.02	15.78	2.64	0.13	0	99.40	76.2
	50.87	0.03	30.07	0	0.53	0	0	13.56	3.60	0.27	0	98.93	66.3
1222.8	48.77	0.48	31.41	0	0.39	0	0	16.33	2.25	0.19	0	99.87	79.3
A	48.85	0	31.41	0	0.51	0	0.05	16.34	2.14	0.19	0	99.56	79.9
1225.7	48.19	0.03	31.53	0	0.57	0	0.03	15.22	2.49	0.14	0	98.21	76.6
1227.5	51.30	0.39	29.98	0	0.52	0.01	0.12	15.66	1.73	0.17	0	99.99	82.7
	49.41	0	31.17	0	0.59	0.01	0.12	16.49	1.66	0.18	0	99.63	83.7
1230.0	54.74	0	30.03	0.03	0.51	0	0.10	13.21	2.74	0.31	0.01	101.68	71.2

Table 3. (Contd.)

Depth, m	SiO_2	TiO_2	Al_2O_3	Cr_2O_3	FeO	MnO	MgO	CaO	Na_2O	K_2O	NiO	Total	Recalculated end-members			
Clinopyroxene													*Fs*	*En*	*Wo*	X_{Mg}
1085.6 H	51.08	1.00	3.80	0.23	8.02	0.19	14.99	21.14	0.31	0.02	–	100.78	13	43	44	76.5
1097.9 G	50.42	0.80	2.12	0.04	11.54	0.39	13.65	20.23	0.36	0.01	–	99.56	19	39	42	67.1
1104.6	51.70	0.65	1.68	0.01	11.63	0.36	14.82	18.59	0.24	0	–	99.68	19	43	38	68.8
1116.5 F	50.14	0.57	1.83	0.03	13.58	0.74	12.12	19.70	0.30	0	–	9.01	24	35	41	60.2
1123.5	50.94	0.74	2.25	0.03	11.32	0.32	14.96	19.18	0.23	0.01	0	99.98	18.4	42.4	39.2	69.7
1130.3	51.64	0.70	2.31	0.07	10.53	0.36	15.02	19.56	0.12	0.01	0	100.32	17.5	42.6	39.9	71.1
1139.2	52.62	0.70	2.04	0.01	11.39	0.40	15.37	18.83	0.27	0.04	0	101.67	18.7	43.2	38.1	69.9
1144.4 E	52.19	0.62	2.36	0.10	8.25	0.22	15.72	20.37	0.11	0.01	0	99.95	13.5	44.8	41.7	76.8
1156.2	51.31	0.65	2.40	0.09	8.78	0.28	15.60	19.75	0.20	0.01	0	99.07	14.6	44.7	40.7	75.4
	52.62	0.42	2.25	0.19	6.99	0.23	16.81	20.34	0.15	0.01	0	100.01	11.4	47.4	41.2	80.6
1164.5	52.34	0.43	2.89	0.45	6.20	0.25	16.08	20.72	0.15	0.01	0	99.52	10.3	46.6	43.1	81.6
	52.64	0.52	3.02	0.57	6.22	0.26	16.56	20.68	0.12	0.02	0	100.61	10.4	47.2	42.4	82.0
1169.2 D	52.53	0.40	1.89	0.20	6.77	0.26	16.98	19.95	0.11	0.01	0	99.10	11.2	48.2	40.6	81.1
1175.0	51.04	0.52	2.51	0.16	6.02	0.18	15.92	21.59	0.11	0.01	0	98.06	9.9	45.6	44.4	82.1
1181.6	52.37	0.70	2.33	0.01	7.48	0.18	16.11	20.63	0.18	–	–	99.99	12	46	42	78.9
1188.3	52.02	0.62	2.51	0.10	8.10	0.22	16.30	20.40	0.34	–	–	100.61	13	46	41	77.7
1194.4	52.70	0.65	2.99	0.42	7.45	0.19	15.97	19.87	0.24	–	–	100.48	12	46	42	78.7
1200.0 C	51.42	0.43	2.74	0.76	6.45	0.15	15.72	20.33	0.28	0.01	–	98.29	11	46	43	80.9
1204.8	51.93	0.52	2.66	0.77	6.02	0.14	16.98	21.21	0.31	–	–	100.54	10	48	42	83.0
	50.67	0.88	2.17	0.32	9.31	0.26	15.22	20.15	–	–	–	99.78	15	43	42	73.9
1208.0	51.83	0.47	2.53	1.21	6.22	0.18	16.33	21.38	–	–	–	100.35	10	46	44	82.0
1209.5	53.03	0.80	2.49	0.92	6.09	0.13	16.33	21.18	0.31	–	–	101.30	10	47	43	82.3
	53.44	0.61	2.64	1.13	6.23	0.19	17.22	19.85	–	0.04	–	101.31	10	49	41	82.6
1218.0 B	52.02	0.54	3.09	0.96	6.43	0.09	16.83	19.58	0.24	0	0.04	99.97	10.5	48.7	40.7	82.2
1221.2	52.06	0.47	2.17	0.63	6.46	0.19	17.31	18.30	0.28	0.02	0.01	98.00	10.9	50.6	38.5	82.2
	52.83	0.47	1.95	0.66	5.33	0.19	18.92	18.89	0.08	0	0.03	99.45	8.8	53.1	38.1	85.9
1227.5 A	52.88	0.63	1.70	0.28	6.34	0.18	16.66	20.20	0.03	0	0.05	98.97	10.6	47.8	41.6	81.9
	54.35	0.43	1.47	0.31	6.54	0.23	17.06	19.99	0.03	0	0.03	100.45	10.8	48.4	40.8	81.8
1230.0	52.78	0.73	2.02	0.19	8.75	0.34	14.89	20.04	0.20	0.01	0.08	100.03	14.8	43.3	41.9	74.4
Orthopyroxene																
1188.3 C	54.72	0.63	1.55	–	16.64	0.41	25.07	2.41	0.05	0.01	–	101.49	26	69	5	72.4
1213.7 B	52.34	0.65	0.96	0.47	13.33	0.43	29.03	1.96	–	–	–	99.17	20	76	4	79.0
1222.8	53.28	0.47	1.19	0.13	13.54	0.34	27.57	2.28	0.04	0	0.08	99.08	21	74	5	78.0
A	53.43	0.40	0.68	0.04	14.85	0.36	27.11	1.93	0.03	0	0.06	98.91	23	73	4	76.1
1225.7	53.88	0.45	0.79	0	16.77	0.41	27.06	1.58	0	0.01	0.08	101.14	25	72	3	73.7
1230.0	55.91	0.47	0.83	0.13	14.21	0.50	26.01	1.97	0	0	0.08	100.12	23	73	4	75.9
Phlogopite, biotite															X_{Mg}	
1097.9 H	36.49	2.49	10.92	0.12	29.96	–	7.28	0.41	0.11	7.93	–	95.86			71.0	
1144.4 E	34.82	2.57	11.96	0.23	29.58	0.31	7.86	0.49	0.08	5.60	0	93.50			69.5	
1164.5 D	38.95	2.87	12.89	0.07	27.82	0.22	7.38	0.25	0.18	9.33	0	99.96			70.1	
1194.4 C	40.85	2.40	11.70	–	16.71	–	14.96	0.27	0.19	9.13	–	96.24			41.4	
1218.0 B	38.76	6.99	12.78	0.15	9.45	0.05	18.47	0	0.47	8.40	0.18	95.77			32.5	
1225.7 A	38.89	5.94	12.63	0.35	9.12	0.01	18.75	0.03	0.34	8.93	0.18	95.25			30.2	

Note: Analyses were conducted on CAMECA and CAMEBAX microprobes at the Institute of the Geology of Ore Deposits, Petrography, Mineralogy, and Geochemistry, Russian Academy of Sciences, analysts T.I. Golovanova and I.P. Laputina. Rock units of the Talnakh intrusion: A—taxitic gabbro-dolerite, B—picritic gabbro-dolerite, C—olivine gabbro-dolerite, D—olivine-bearing gabbro-dolerite, E—olivine-free gabbro-dolerite, F—gabbro-diorite, G—prismatically granular gabbro-dolerite, H – ataxitic olivine-free gabbro-dolerite, marginal near-contact gabbro-dolerite, and volcanic breccia. Dashes mean not analyzed.

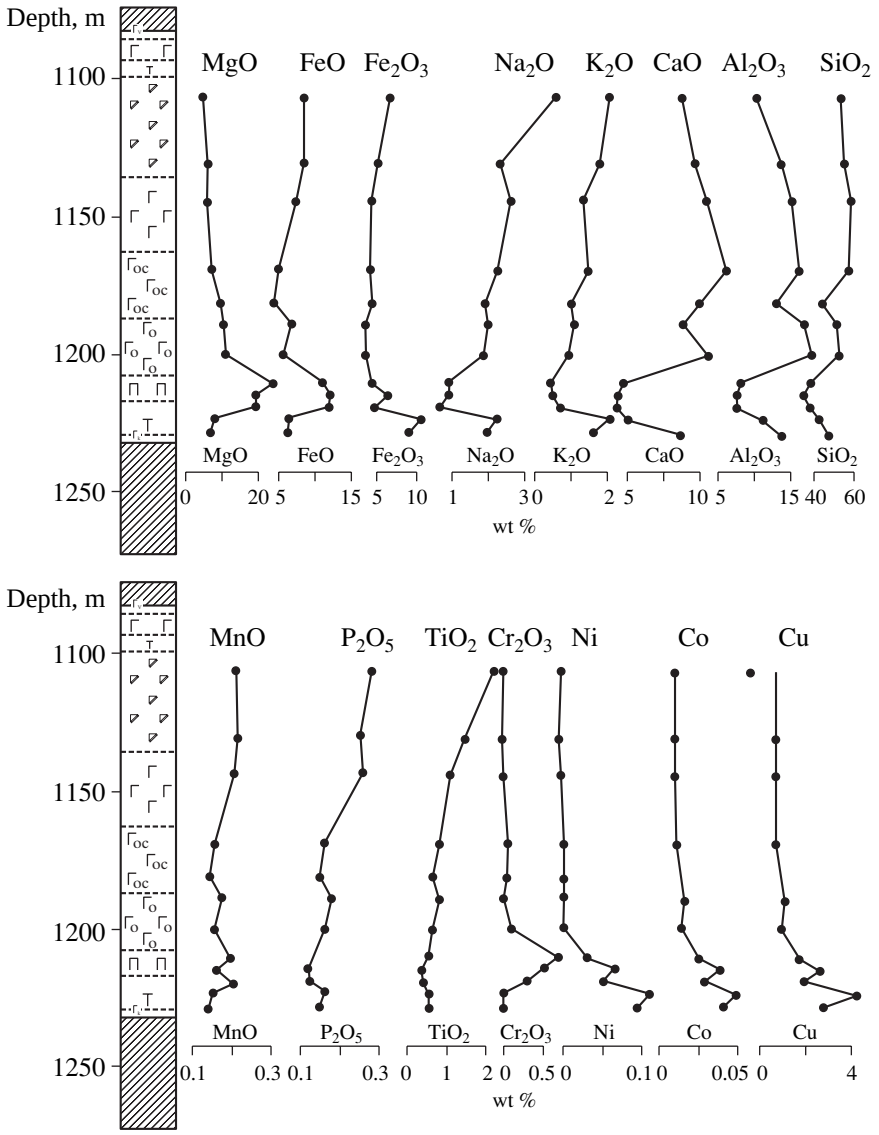

Fig. 3. Variations in the concentrations of major and trace elements in the vertical section of the Talnakh intrusion (Hole OUG-2).

massif is shown in Fig. 3. The analysis of these data testifies for the different behavior styles of major and ore-forming elements, which can be classified into the following groups: (1) MgO and Cr_2O_3; (2) FeO and Fe_2O_3; (3) CaO, Al_2O_3, and SiO_2; (4) TiO_2, Na_2O, K_2O, and P_2O_5; and (5) Co, Ni, and Cu.

(1) The variations in the MgO concentration over the section are determined mainly by the amounts of *Ol* in the rocks and by the Mg# of this mineral. The overall range of variations in the MgO concentrations is 5.11–22.41 wt %. The highest concentrations are characteristic of the unit of picritic gabbro-dolerites, whose uppermost one-third is marked by an absolute maximum in the MgO concentration. The concentration of this oxide in the rocks decreases upward and downward from this ultrabasic unit. It should be also noted that, in some sections of the intrusion, *Ol*-enriched rocks appear in the upper inner-contact zone and cause a second maximum in the MgO concentration.

The distribution curve of Cr_2O_3 virtually fully follows variations in the concentration of MgO (Fig. 3), with significant differences in the concentrations of the two component observed only in the upper part of the unit of olivine gabbro-dolerites. The relative minimum in the Cr_2O_3 concentration in this layer is explained by the strong decrease in the content of Cr-magnetite in the rock at a gradual upward decrease in the olivine content. The Cr_2O_3 concentration ranges over the section of the massif from the detection limit (<0.007 wt %) in the upper taxitic gabbro to 0.77 wt % in the picrites and has an absolute maximum in the upper part of the picrite unit. These units also contain the most chromic clinopyroxene (Fig. 2) and large amounts (mainly in the form of segregations) of Cr-magnetite and chromite.

Table 4. Illustrating examples of calculations of the silicate constituent of rocks from the Talnakh intrusion (Hole OUG-2)

Component	Picritic gabbro-dolerite, OUG-2/1213.7		Taxitic gabbro-dolerite, OUG-2/1230	
	1	2	3	4
SiO_2	37.66	45.08	43.34	51.57
TiO_2	0.4	0.48	0.54	0.64
Al_2O_3	7.9	9.46	14.01	16.67
Fe_2O_3	6.59	–	8.76	–
FeO	12.52	14.06	6.75	8.61
MnO	0.18	0.22	0.15	0.18
MgO	18.77	22.47	6.64	7.90
CaO	5.01	6.00	9.22	10.97
Na_2O	0.88	1.05	1.94	2.31
K_2O	0.32	0.38	0.79	0.94
P_2O_5	0.57	0.13	0.034	0.17
Cr_2O_3	0.11	0.68	0.14	0.04
H_2O^-	0.22	–	0.24	–
H_2O^+	2.96	–	1.79	–
Ni	0.53	–	0.59	–
Co	0.03	–	0.03	–
Cu	1.58	–	1.79	–
S	4.23	–	4.85	–
CO_2	0	–	0	–
F	<0.05	–	0.06	–
Total	100.47	100.00	101.66	100.00

Note: (1, 3) Original compositions; (2, 4) calculated compositions (all Fe is given as FeO).

Upward and downward from the picrite unit, the concentrations of these oxides and Cr_2O_3 in clinopyroxene decrease, and, as a consequence, the rock become progressively depleted in Cr_2O_3.

(2) FeO and Fe_2O_3 are characterized by similar distribution trends (Fig. 3). The maximum concentrations of these oxides (7.6 and 11. 45 wt %, respectively) were encountered in the picrites, in which these values are explained by an increase in the proportion of *Ol* and *Opx* to *Pl*, and in the gabbro-diorites of the upper part of the section, in which they are accounted for by elevated (up to 10–15%) concentrations of titanomagnetite. The lowest concentrations of iron oxides fall to the contact zone between the picrites and olivine gabbro-dolerites.

(3) The highest concentrations of CaO and Al_2O_3 (12.21 and 17.32 wt %, respectively) are spatially restricted to the olivine and olivine-bearing gabbro-dolerites, which is explained by the enrichment of plagioclase in these rocks and the high Ca# (up to An_{84}) of this mineral. A similar situation was observed in the plagioclase-rich rocks: taxitic gabbro-dolerites and anorthite leucogabbro from the lower and upper units. The CaO and Al_2O_3 concentrations in the upper taxites somewhat decreases, which is correlated with an increase in the albite concentration of the plagioclase. The concentrations of these elements in the picritic gabbro-dolerites strongly decrease (to 4.96 and 7.75 wt %, respectively) owing to the overall decrease in the *Pl* content at its constant Ca#. The behavior of SiO_2 in the lower part of the intrusion is analogous to those of CaO and Al_2O_3, and, starting from the unit of olivine gabbro-dolerites, the silicity of the rocks practically does not change.

(4) Phosphorus, titanium, and alkalis display a tendency of gradual enrichment toward the roof of the intrusion, i.e., exhibit trends opposite to those of CaO and Al_2O_3. All incompatible elements are characterized by slightly elevated concentrations near the bottom of the massif, with each element showing small local maxima and minima in the section. For example, an increase in the Na concentration in the upper part of the succession is related to a decrease in the Ca# of *Pl* and, to a lesser degree, secondary alterations of the rocks. An analogous situation with Ti is explained by the appearance of titanomagnetite in the upper part of the sequence.

(5) The enrichment of ore components, Ni, Co, and Cu, was related mainly to sulfides, a fact that predetermined the maximum concentrations of these metals in the lower mineralized derivatives (picritic and taxitic gabbro-dolerites). Note that compared with Co and Cu, the Ni concentration is characterized by a smoother decrease over the section, a phenomenon that is possibly explained by relatively high Ni concentrations in olivine and the monotonous variations in the content of this mineral.

Taking into account the task of determining the initial parameters of the Talnakh magma, our study was focused mainly on rocks from the lower portion of the massif, starting from the near-contact taxites to picritic gabbro-dolerites with the highest concentrations of MgO. These units are characterized by significant variations in the rock chemistry, with the concentration of components changing as follows: SiO_2 by approximately 5 wt %, Al_2O_3 by approximately 10 wt %, MgO by approximately 15 wt %, and FeO_{tot} and CaO by approximately 7 wt %. These variations over the vertical section are systematic and may have been caused by the redistribution of crystals (mainly intratelluric) at the insignificant fractionation of the parental magmatic melt (Dneprovskaya *et al.*, 1987). As follows from the foregoing sections of this paper, this situation is genetically informative and meets the conditions formulated above for the applicability of geochemical thermometric techniques.

SIMULATION OF PHASE EQUILIBRIA

In order to carry out thermometric calculations, we used the chemical compositions of rocks recovered by

Hole OUG-2 (Table 2) and Holes KZ-1713 and KZ-1799 to the north of it (Czamanske *et al.*, 1995). The employment of additional data was caused by the need to enhance the representativeness of the petrological material and the intention to rely on data from relatively closely spaced sections (Fig. 1). Their spatial closeness let us suggest that there were only insignificant differences between the compositions of melts entrapped by the rocks of lower units, for which no significant lateral geochemical heterogeneity was detected (Dneprovskaya and Dneprovskii, 1988). Thus, we used for the calculations only the compositions of picritic (n = 13) and taxitic (n = 6) gabbro-dolerites: eleven samples from Hole KZ-1799, seven from Hole KZ-1713, and five from Hole OUG-2.

Selection of Starting Compositions

Recent versions of the COMAGMAT program enable one to simulate melt–crystal equilibria that involve five silicates (*Ol*, *Pl*, *Aug*, *Pig*, and *Opx*) and two oxides (Ti-*Mt* and *Ilm*) but no crystallizing sulfides. An attempt to use this model in order to calculate phase equilibria in rocks with significant amounts of sulfides may result in changes in the configurations of the fields of some minerals and shift in the model lines for the melt evolution. Because of this, the original chemical compositions should be recalculated to determine the amounts of FeO in the silicate matrix based on the overall sulfur and base-metal concentrations in each individual sample. The recalculation technique implies that Cu and Ni are contained only in chalcopyrite and pentlandite, respectively, and it is assumed that the proportion of Ni accommodated in olivine is insignificant and does not principally affect Fe balance between the sulfide and silicate constituents of the rock.

The calculation succession involves (1) the assay of the bulk amounts (in wt %) of chalcopyrite and pentlandite in the rocks on the basis of data on their actual compositions and the concentrations of Cu and Ni in the rock; (2) the calculation of the amounts of S contained in these minerals; (3) the calculation of the excess S (based on the data of a chemical analysis) that should be assigned to pyrrhotite; (4) the calculation of the FeO concentration in the silicate matrix as a difference between the whole-rock and "sulfide" FeO_{tot} concentrations; and (5) the normalization of the composition calculated to 100 wt % anhydrous residue. The amounts of iron in sulfides were computed from the following compositions of minerals: chalcopyrite was calculated as stoichiometric $CuFeS_2$ (i.e., Cu = 34.64, Fe = 30.42, and S = 34.94 wt %); for other minerals, their averaged microprobe analyses (obtained for disseminated ores from Hole OUG-2) were taken. In accordance with these data, we assumed the following average compositions (wt %) of pentlandite: Ni = 32, Fe = 34, and S = 34 for the picritic gabbro-dolerites and Ni = 35, Fe = 31, and S = 34 for taxitic gabbro-dolerites. The average pyrrhotite compositions (wt %) are Fe = 61, S = 39 for picrites and Fe = 60, S = 40 for taxites. Table 4 presents examples of the calculations made for two samples from Hole OUG-2. The whole sampling of compositions of the silicate constituent of the rocks used in the calculations of phase equilibria is available from the authors.

Additionally, we conducted a series of calculations for three compositions that were the weighted mean assays for rocks of the Talnakh intrusion (Table 5). They were based on the data of M.B. Dneprovskaya on 29 holes (Dneprovskaya *et al.*, 1987), the data of T.E. Zen'ko and V.A. Fedorenko *et al.* on Holes KZ-1799 and KZ-1713 (Czamanske *et al.*, 1995), and our results on rocks from Hole OUG-2 (Table 2). All of the cited compositions characterize weighted mean estimates for the silicate constituent of the Talnakh rocks, which were calculated by the same techniques as those used for individual samples.[1] These initial compositions are interesting because they potentially contain analogous information on the intrusion temperature and on the composition of the intratelluric phases and magmatic melt, which is "recorded" in the bulk compositions of rocks from lower units. When an ideal sheet-shaped body is considered, these compositions should not be principally different and, in fact, represent the composition of the parental magma [see Eq. (1)]. In reality, it is impossible to correctly evaluate the weight proportions of all rock varieties that compose both continuous units and small bodies, lenses, etc. Because of this, we consider these weighted mean compositions to be model systems, which, perhaps, not always correspond to the parental magma but are nevertheless useful to check the correctness of the geochemical thermometric results obtained for the actual igneous rocks.

[1] The composition proposed by M.B. Dneprovskaya includes data on the Kharaelakh Massif, a fact that somewhat diminishes its significance for the Talnakh intrusion. However, the relative volume of information on the Kharaelakh rocks in this sampling is insignificant, and this makes it possible to utilize this assessment in further genetic reconstructions. Using the compositions of rocks from Holes KZ-1799 and KZ-1713, we first constructed a generalized cross section with due allowance for the overlap of the core material (Czamanske *et al.*, 1995; the primary analytical materials were made available by courtesy of V.A. Fedorenko). Judging from our observations and known generalizations by other researchers (Zolotukhin *et al.*, 1975; Ryabov *et al.*, 2000), this cross section is not very typical of the Talnakh intrusion, because it includes a relatively thick (up to 30 m) unit of quartz diorite, which either is absent from other cross sections or is not as thick. In calculating the weighted mean compositions of rocks from Holes 1799 and 1713, the thickness of this unit was intentionally decreased to 5 m. In estimating the weighted mean composition for the reference Hole OUG-2, we rejected the uppermost Sample 1104.6 (Table 3) because of its anomalously high concentration of Na_2O (the composition of the near-roof part was approximated over a 25-m interval because of greater distances between the sampling sites, and this significantly affected the calculated average alkalinity of the rocks).

Table 5. Different estimates for the weighted mean composition of the silicate constituent of rocks from the Talnakh intrusion

Component	1	2	3
SiO_2	47.60	48.20	49.05
TiO_2	1.11	0.85	0.89
Al_2O_3	14.15	15.30	14.99
FeO	12.36	12.32	11.15
MnO	0.22	0.19	0.20
MgO	11.57	9.98	10.58
CaO	10.25	10.43	10.10
Na_2O	1.92	1.86	2.06
K_2O	0.56	0.58	0.65
P_2O_5	0.12	0.20	0.18
Cr_2O_3	0.13	0.10	0.14

Note: (1) Holes KZ-1799 and KZ-1713 (Czamanske *et al*., 1995); (2) average for 29 holes (Dneprovskaya *et al*., 1987); (3) for Hole OUG-2 (our data). All Fe is given as FeO.

Calculation Conditions

An important aspect of geochemical thermometry is specifying the pressure and redox conditions of the parental magma intrusion. While studying the outer-contact zones of the Noril'sk-I intrusion, we determined that the host limestone contains monticellite rocks, and this allowed us to determine that the complex had been intruded under conditions of the gehlenite–monticellite depth facies (Godlevskii, 1959). This estimate is consistent with data on the lithostatic load created by rocks overlying intrusions of the Noril'sk type (500–1000 bar; *Magnezial'nye bazity…*, 1984). In compliance with this information, we calculated the crystallization equilibria for pressure of 0.5 kbar.

The estimates for the oxygen fugacity are less definite. They are usually based on the whole-rock Fe_2O_3/FeO proportion, which should depend, by analogy with melts, on the temperature, f_{O_2}, and composition. Calculations that were conducted for the rocks of magnesian intrusions in the northwestern Siberian Platform and make use of the simplest relations of Fudali (1965) for 1200°C yielded $\log f_{O_2}$ values from –7.2 to –8.2 (*Magnezial'nye bazity…*, 1984). This interval overlaps with the range of buffer equilibria from approximately NNO + 0.5 to QFM. In modeling the crystallization trajectories, we assumed that the conditions were more reduced, QFM – 0.5, because it is known that the Fe_2O_3/FeO ratios of rocks are usually disturbed by surface oxidation and the respective Fe_2O_3/FeO values become overestimated compared with the actual values of the magmatic melts (Carmichael and Ghiorso, 1990).

In calculations by the method of geochemical thermometry, it is necessary to specify the water concentration of the parental melts, which are the full melting products of certain rocks, in our case, taxitic and picritic gabbro-dolerites. No such melts exist in nature, but their compositions should be used as the starting points in the calculations of the equilibrium crystallization trajectories (see the section devoted to the fundamentals of geochemical thermometry techniques). Hence, the initial water concentration of the melts of the taxitic and picritic gabbro-dolerites was taken to be equal to 0.1 wt %, a value that ensured melt undersaturation with respect to water at the assumed pressure and 0–70% crystallinity (Al'meev and Ariskin, 1996). This condition implies that the Talnakh rocks contain no primary magmatic amphibole and is consistent with the insignificant concentrations of water-bearing phases, for example, biotite (Ryabov and Zolotukhin, 1977). Phase equilibria were calculated for each sample successively, as the crystallinity of the melt progressively increased, with a step of 1 mol % crystallinity. The maximum crystallinity of the model systems did not exceed 80% (20% captured liquid).

Results of Geochemical Thermometry

Crystallization order. For 19 of the 23 calculated trajectories, the crystallization of excess *Ol* was determined over the temperature interval of 1250–1540°C (Fig. 4). The second crystallizing phase was *Pl* (its minimum melting temperature is 1255°C), and the third was clinopyroxene (*Aug*). In four case, cotectic *Ol* + *Pl* crystallization was identified at temperatures of ~1200–1235°C, and the next crystallizing mineral was augite. The initial crystallization temperature of augite never exceeded 1189°C. The character of textural relations of *Cpx* with *Ol* and *Pl* observed in the taxitic and picritic gabbro-dolerites suggests the absence of *Cpx* from the primary liquidus mineral assemblage (see above), and, hence, the calculated value of ~1190°C can be regarded as the lower limit for the probable temperature of the parental magma emplacement.

The anomalously high liquidus temperatures of high-Mg picritic gabbro-dolerites (T > 1450°C) testify to the cumulative nature of these rocks, which were produced by the accumulation of olivine crystals. This follows from the calculated composition of the high-temperature olivine (91–92% *Fo*), which is much more magnesian than the most primitive *Ol* (Fo_{82}) encountered in the rocks of the lower units. It is interesting to analyze the distribution structure of the liquidus temperatures of olivine (Fig. 4). Note that the absence of calculated temperatures in the range of ~1300–1450°C causes the apparently bimodal character of the histogram. We believe that this is a direct implication of the contrasting character of MgO distribution (and also the distribution of *Ol*) over the section of taxitic and picritic gabbro-dolerite units (Fig. 3). This fact suggests that the parental magma parameters should be searched for at temperatures below ~1300°C.

In this connection, it is expedient to return to the initial crystallization of plagioclase (Fig. 4). The highest calculated melting temperatures of this mineral are approximately 1250°C, but these evaluations pertain to the rocks with small amounts of excess *Ol* and, perhaps, *Pl*. Apparently, the actual crystallization temperatures of plagioclase could not exceed the liquidus values for the subcotectic rocks, when *Ol* and *Pl* started to crystallize concurrently. According to our calculations, these temperatures were 1200–1235°C. Hence, provided the parental magmatic melt was saturated with respect to both *Ol* and *Pl* but undersaturated with respect to *Aug*, the probable temperature range of the parental magmas should be constrained to 1190–1235°C.

The considerations and evaluations presented above were based on the crystallization succession of the melts of the taxitic and picritic gabbro-dolerites and a textural interpretation of these rocks, which implies that clinopyroxene was absent from and plagioclase was present in the primary liquidus assemblage. Genetic models of this type inevitably involve uncertainties. The correctness of the assays could be justified by an intersection of (or closer spacing between) the calculated evolutionary lines for the melt near 1200°C.

Estimated composition of the parental melt. Figure 5 shows the compositional trends of melts, calculated for the samples as functions of temperature over the interval of 1350–1120°C. The seventeen lines demonstrated in the plot represent, with a high degree of confidence, a single set of cotectics, in spite of the significant differences between the initial compositions. The other six trajectories demonstrate a wider scatter in the FeO and SiO_2 concentrations of the melts (the causes of this phenomenon remain still unclear), and, thus, they were excluded from further consideration.[2] The plot also shows the evolution trajectory of melt during the equilibrium crystallization of the weighted mean composition of the Talnakh intrusion (based on our data on Hole OUG-2; Table 5).

These data demonstrate that the convergence and intersections of the model lines can be reliably enough identified based on the concentrations of Al_2O_3 and FeO (and, to a lesser degree, also SiO_2 and TiO_2) and are restricted to the temperature interval of 1180–1220°C. These temperature and compositional intervals also include the trajectory for the weighted mean composition. Hence, the results of geochemical thermometry allowed us to estimate the temperature of the parental Talnakh magma at 1200 ± 20°C (with an error slightly smaller than those of geothermometers used in the COMAGMAT program). Table 6 lists an average estimate for this magmatic melt, which was calculated with the use of the 17 compositions, each of which is represented by an individual model line at 1200°C. Apparently, this composition can be classed with typical tholeiitic ferrobasalt somewhat enriched in K. It contains approximately 8 wt % MgO and, thus, is notably more magnesian than the average composition of the "normal" flood basalt in the Siberian Platform (Table 1) but still does not attain the values of 10–12 wt % MgO that should determine, according to Zolotukhin *et al.*, the picrite-basaltic character of the parental melt of the Siberian flood basalts (*Magnezial'nye bazity…*, 1984).

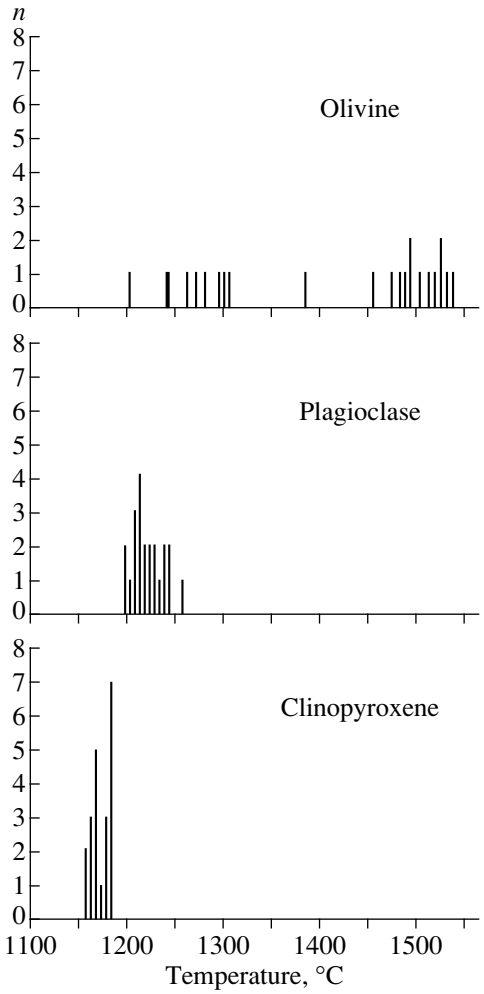

Fig. 4. Histograms of the temperatures of the beginning of crystallization for the main rock-forming minerals of the taxitic and picritic gabbro-dolerites (computer simulation results on phase equilibria).

Chemistry of minerals in the original assemblage. In the section devoted to the method of geochemical thermometry, we pointed out that it is based on the assumption of the equilibrium character of component distribution between minerals and melt in the assemblage original for each rock. This means that, at small differences between the estimated compositions of the intercumulus melts, the calculation results should yield similar estimates for the original composi-

[2] The discrepancies are most probably caused by the superposition of analytical uncertainties (including the corrections for sulfides) and the calculation errors with the COMAGMAT computer model. However, it cannot also be ruled out that these deviations are of genetic nature and were caused by the allochemical nature of the petrogenetic process or their partial recrystallization.

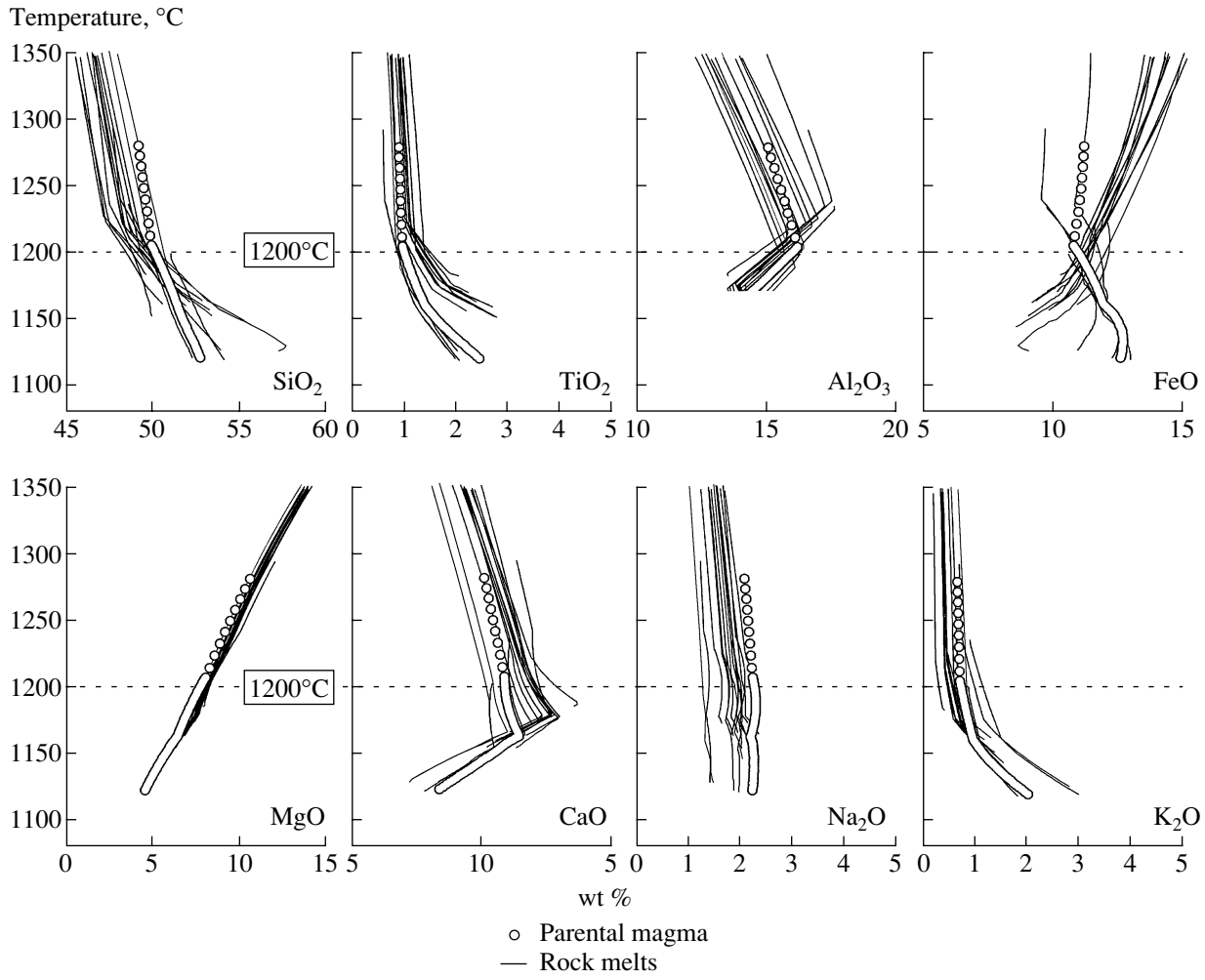

Fig. 5. Estimated temperatures and composition of the parental melt of the taxitic and picritic gabbro-dolerites in the upper zone of the Talnakh intrusion.

The desired characteristics are determined by the intersection point (or the area of maximum convergence) of the model evolutionary trends for the silicate liquid during the equilibrium crystallization of melts (data for individual samples). The trend for the parental magma corresponds to composition 3 in Table 5.

tions of minerals at the determined formation temperature of the rock. Taking into account that all of the 17 trajectories portrayed in Fig. 5 for 1200°C suggest an *Ol* + *Pl* assemblage, one can evaluate the compositions of these liquidus phases and assume them as the original characteristics of the Talnakh magma. Figure 6 demonstrates the compositional evolution of olivine and plagioclase in each of the samples and the uncertainty intervals for the simulation results at 1200°C. The calculations for the average values at this temperature yield 81.3 ± 1.1 mol % *Fo* in *Ol* and 80.5 ± 2.4 mol % *An* in *Pl*. These values are in good agreement with microprobe analyses of the minerals, which demonstrate that the maximum Mg# of *Ol* in the taxitic gabbro-dolerites corresponds to $Fo_{82–83}$, and the highest temperature plagioclase contains no more than 83% *An*.

Phase composition of the magma parental for the rocks of lower units. A noteworthy feature of geochemical thermometry is its ability to assay the phase proportion of the parental magma [F_j^{sus} and F_l in Eq. (1)] and the proportions of cumulus grains, F_j^{cum}, and melt F_l^{int} [see Eqs. (2) and (3)] in the original cumulates, from which the rock eventually crystallized. These proportions can be found by tackling the problem of thermodynamic equilibrium for each sample at the determined temperature of rock formation. The phase parameters of the parental magma can be estimated in an analogous manner, i.e., from the constructed trajectories of equilibrium crystallization for weighted mean compositions. Table 7 presents the full phase and chemical characteristics of the melt–crystal associations, which represent, at 1200°C, the aforementioned models for the composition of the Talnakh intrusion (Table 5). As is seen from these data, the *Ol* + *Pl* (with the predominance of *Ol*) cotectic assemblage is identified in all instances, with the overall percentage

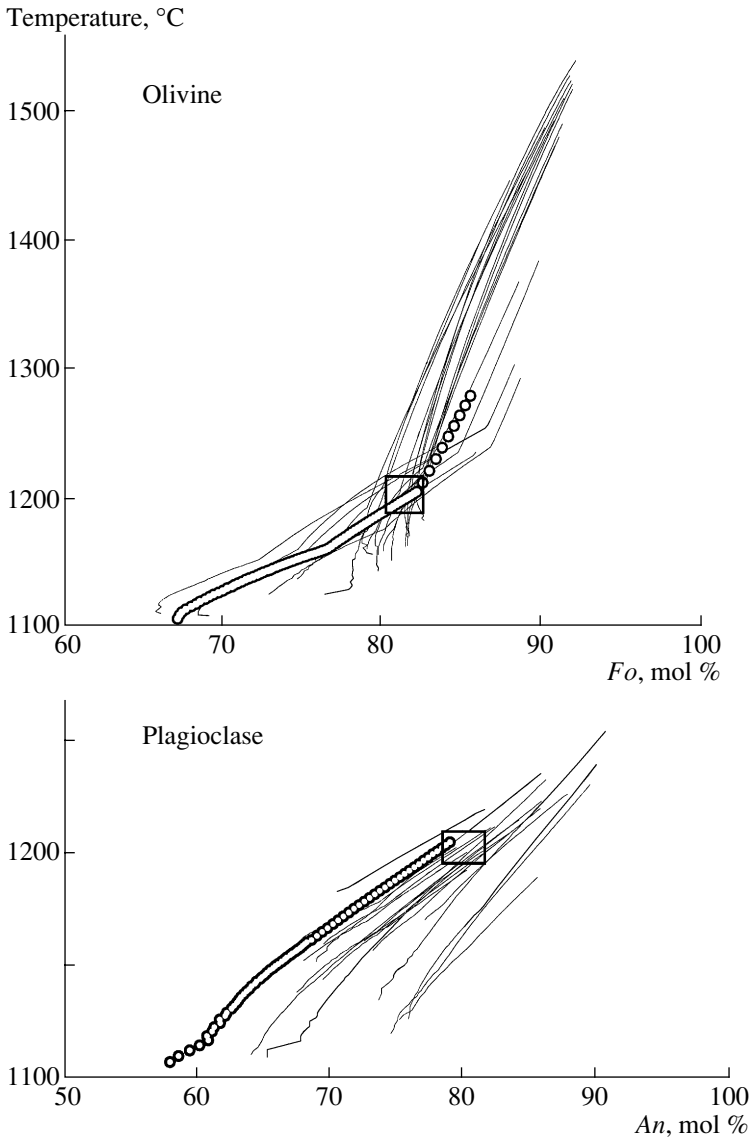

Fig. 6. Calculated evolutionary trends for olivine and plagioclase compositions during the equilibrium crystallization of taxitic and picritic gabbro-dolerite melt of the Talnakh intrusion.

Circles represent data on the parental magma (Table 5, composition 3); rectangles show the uncertainty intervals for the simulation results at 1200°C.

of intratelluric phenocrysts in the magma during its intrusion amounting to 10.8–14.0 wt %. The composition of the liquid constituent of the parental magma are also consistent with the estimate obtained on the contact gabbro-dolerites (Table 6).

Figure 7 presents the model distribution of cumulative *Ol* + *Pl* over the generalized section for the lower part of Holes KZ-1799 and OUG-2. The thicknesses of the picritic and taxitic gabbro-dolerite units in this section is given as percent of the overall thickness of the intrusive rocks penetrated by each of the holes. The upper pair of plots illustrates the relationships between the calculated amounts of original *Ol* crystals and the actual MgO and Ni concentrations of the rocks. Apparently, our geochemical thermometric data point to a gradual increase in the amounts of cumulus crystals from a few percent near the lower contact of the taxitic gabbro-dolerites to 50–60% in the upper part of the picrite unit. It should be taken into account that the strong correlation between the chemical and modal parameters cannot be regarded as a direct validation of the cumulus hypothesis, because the *Ol* contents were calculated from the chemical compositions by the solution of the inverse problem. An independent proof could be provided by data on Ni, but the presence of sulfides obscures a correlation between this element and the model amounts of olivine.

Table 6. Composition of the parental magmatic melt compared with the compositions of the near-contact gabbro-dolerites of the Talnakh Massif and some volcanic flood basalts from the northwestern Siberian Platform

Component	Talnakh intrusion			Average compositions of volcanic flood basalts		
	model melt at 1200°C (n = 17)	near-contact gabbro-dolerite		Mokulaevskaya Formation		flood basalts of the Putorana Plateau (n = 300)
		average composition (n = 2)	hole KZ-1799/1341.9	Mk_1	Mk_2	
	1	2	3	4	5	6
SiO_2	49.44 (0.71)	47.29	49.89	49.89	49.87	49.89
TiO_2	1.20 (0.22)	1.67	1.24	1.21	1.21	1.30
Al_2O_3	15.44 (0.46)	14.95	15.76	15.45	15.50	15.53
FeO	11.43 (0.66)	13.73	11.69	11.59	11.39	12.04
MnO	0.22 (0.02)	0.21	0.23	0.17	0.19	0.19
MgO	8.06 (0.19)	7.50	7.44	6.80	7.22	7.30
CaO	11.53 (0.71)	11.52	10.68	12.34	12.14	11.43
Na_2O	1.82 (0.26)	2.11	1.98	2.17	2.15	1.93
K_2O	0.69 (0.22)	0.89	0.92	0.22	0.17	0.29
P_2O_5	0.19 (0.04)	0.12	0.15	0.15	0.15	0.12

Note: Numbers in parentheses are standard deviation (1σ) values; (2) Dodin and Batuev, 1971 (see Table 1); (3–5) *Geology and Ore...*, 1994; Mk_1—aphyric basalts of the Mokulaevskaya Formation, unit 1, Mk_2—glomerophyric basalts of the Mokulaevskaya Formation, unit 2); (6) Nesterenko *et al.*, 1991. All Fe is given as FeO. Compositions are normalized to 100%.

Analogous distributions are shown for the model plagioclase and alumina (Fig. 7). They indicate that the amounts of *Pl* crystals (which are supposedly intratelluric) entrapped at the lower front vary from 10 to 30% in the taxites and strongly decrease, to 2–5%, in the picrites. This is correlated not only with Al_2O_3 but also with the distribution of Sr, whose concentrations were not taken into account in the geochemical thermometric simulations. This correspondence can be treated as an independent criterion pointing to the presence of early plagioclase crystals in the parental Talnakh magma.

Table 7. Chemical and phase composition of the parental magma of the Talnakh intrusion based on computer simulation data

Component	1	2	3
Composition (wt %) of the parental melt at 1200°C			
SiO_2	48.75	48.98	50.08
TiO_2	1.30	0.95	1.00
Al_2O_3	15.42	15.74	15.88
FeO	12.00	12.35	10.94
MnO	0.22	0.19	0.20
MgO	7.94	7.91	7.81
CaO	11.43	11.01	10.90
Na_2O	2.16	1.99	2.25
K_2O	0.65	0.64	0.74
P_2O_5	0.14	0.22	0.21
Phase composition (wt %) of the parental melt			
Melt	86.0	89.2	88.5
Ol	11.3 ($Fo_{80.3}$)	7.0 ($Fo_{79.8}$)	8.6 ($Fo_{81.8}$)
Pl	2.7 ($An_{78.1}$)	3.8 ($An_{80.1}$)	2.9 ($An_{78.5}$)
Ol + *Pl*	14.0	10.8	11.5

Note: (1–3) Different variants of the weighted mean composition of the Talnakh intrusion (see Table 5); *Ol* + *Pl* is the overall fraction of intratelluric phenocrysts during magma intrusion.

It is also interesting to compare the evolution of the amounts of complementary magmatic melts, which were calculated for each rock from thermometric data, and the distribution of incompatible elements. These relations are demonstrated in the lower plots of Fig. 7 for P, Y, Sm, La, and Th. For both holes, there seems to be a concurrent decrease in the amounts of melt from 70–85% in the upper portion of the taxites to 45–50% in the picrites. This decrease is strongly correlated with the distribution of P_2O_5, Y, Sm, La, and Th, whose concentrations also decrease by factors of 2–2.5 toward the upper part of the picrite unit. Data on incompatible elements are independent in our approach, and this also testifies to an important role of the proportions of the parental melt and crystals in the formation of the chemical composition of the lower contact units.

DISCUSSION

The model simulations presented above pertain to the most complicated (in the structural sense) zone of the Talnakh intrusion, the lower units of near-contact, taxitic, and picritic gabbro-dolerites, whose genesis was discussed over several years and which constantly

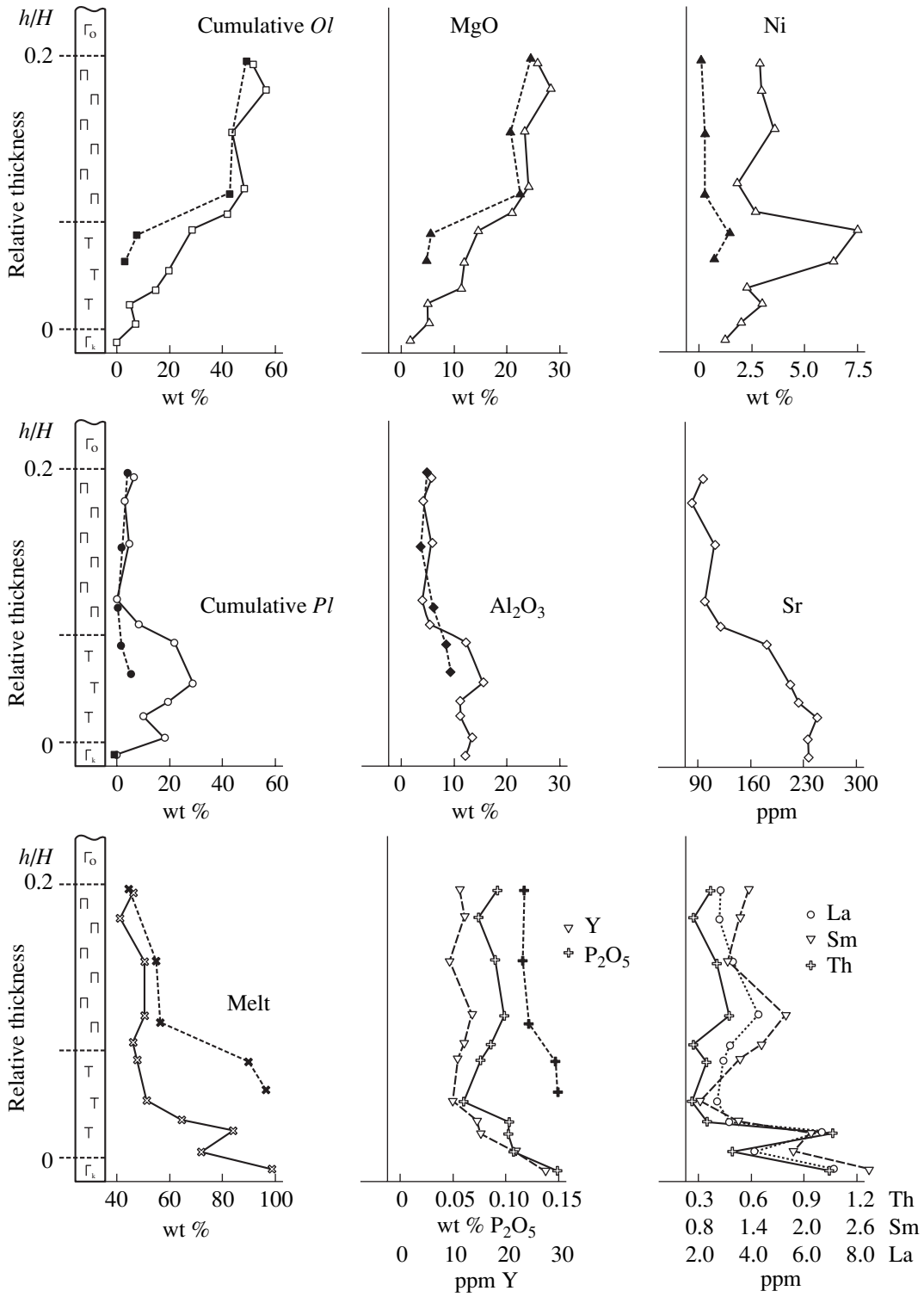

Fig. 7. Model distribution of the amounts of cumulus phases and melt compared with the concentrations of some major and trace elements.

Concentrations of elements are given in accordance with chemical analyses of the picritic and taxitic gabbro-dolerites from Holes OUG-2 (Table 2) and KZ-1799 (Czamanske, 1995). Open symbols represent data on Hole KZ-1799, solid symbols are data on Hole OUG-2.

attracted much attention because of their ore-generating role. This follows from several petrological and geological observations that are usually put forth as arguments against hypotheses proposed for the origin of layered intrusions by means of crystallization differentiation. These petrological and geological features are as follows: (1) inconsistencies between the compositions of contact gabbro-dolerites and the weighted mean composition of the intrusion; (2) the "suspended" position of picritic gabbro-dolerites in the magmatic succession; (3) traces of "magma flow" in the picrite units; (4) sharp boundaries between the picritic gabbro-dolerites and overlying olivine gabbro-dolerites; (5) tapering of the picritic units toward the peripheral parts and weak correlations between their thicknesses and that of the intrusion as a whole; (6) the restriction of taxitic gabbro-dolerites to the bottom of the intrusion; and (7) the presence of "wandering" leucogabbro bodies in the magmatic sequence and the unsystematic increase in the thicknesses of taxitic gabbroids toward the peripheral parts of the intrusive body.

In order to interpret these and several other facts, a great variety of hypotheses was proposed, which included (1) fluid–magmatic liquid immiscibility with the origin of picritic units from an individual picritic magma, which was segregated from the bulk of the parental magmatic melt (Ryabov *et al.*, 2000); (2) the relatively early development of the taxitic gabbro-dolerites and leucogabbro because of the still earlier intrusion of *Pl*-enriched magmatic mush into the chamber (Likhachev, 1965, 1978); (3) the later origin of the taxitic units as a consequence of magmatic and postmagmatic leucocratization and sulfurization of the rocks of the Main Layered Series (Zolotukhin, 1997); (4) the origin of the taxitic gabbro-dolerites under the effect of transmagmatic fluids on the gabbro-diorites (Zotov, 1979, 1989); and others. Our reconstructions of the formation conditions of the taxitic and picritic gabbro-dolerites and the chemical and phase characteristics of the Talnakh magma provide a consistent solution of most of the problems formulated above within the guidelines of the concept of heterogeneous parental magmatic system with allowance for the sorting and accumulation of intratelluric material.

The main results of the conducted analysis include the good agreement (within the accuracy of the method) between the composition of contact gabbro-dolerites and the calculated composition of the parental melt (Tables 6, 7). This testifies to the realistic character of our models, because the origin of the composition of the contact zones has not been adequately interpreted as of yet. Conceivably, insignificant amounts of intratelluric phenocrysts contained in the rocks can be accounted for by the known effect of pressing of crystals away from contact zones as the magma flows and fills intrusive chambers (Naslund and McBirney, 1996; Sharapov *et al.*, 1997). From the viewpoint of regional magmatism, the parental magmatic melt has a typical tholeiitic composition, which corresponds to ferrobasalt slightly enriched in K_2O. Comparison between the major-component composition of the parental melts with that of the volcanic flood basalts of the Noril'sk district reveals the closeness of the former to the late-stage volcanics of the Siberian Platform, particularly to the aphyric and glomerophyric basalts of the Mokulaevskaya Formation (Mk_1 and Mk_2, respectively; *Geology and Ore…*, 1994). Since we compare only the composition of the melt (but not the magma as a whole), it seems to be more correct to compare it with aphyric varieties, although they are less magnesian than the glomerophyric basalts. It is also interesting to note that the composition of the parental melt is close to the average compositions of basalts in the Putorana Plateau, which account for more than 90 vol % of the plateau basalts of the Siberian Platform (Nesterenko *et al.*, 1991; Table 6).

Another important result is concerned with the original *Ol* + *Pl* cotectic nature of the Talnakh magma. This idea is not new: the occurrence of early *Pl* and *Ol* in the Talnakh magma was suggested by Korovyakov (1963), Oleinikov (1979), Zolotukhin *et al.* (1975, 1997), and other researchers. This problem was considered in much detail by Likhachev (1965, 1977, 1997), who has also arrived at the conclusion that the intruded magma had been saturated with respect to *Ol* and *Pl*. It is admitted that the gravitation-induced segregation of minerals occurred when the magma ascended to the surface, so that the chamber was initially filled with plagioclase-rich mush, which was then pushed away and forced to the peripheral parts of the massif by the main volume of melt, which was enriched in olivine. Within the guidelines of this hypothesis, the taxitic gabbro-dolerites and leucogabbro were produced by early batches of the magma, a hypothesis that explains the position of these rocks near the bottom and their occurrence as "wandering" bodies among other gabbro-dolerites. Our geochemical thermometric results do not contradict this cotectic interpretation but demonstrate that the average Talnakh magma contained roughly 3% intratelluric *Pl* (Table 7). This estimate should somehow agree with the amounts of leucogabbroids, which are unevenly distributed over the volume of the Talnakh intrusion. However, the method used in our research cannot explain the genesis of the early phases of olivine and, particularly, plagioclase, for which the compositions An_{90} and more calcic were reported. It is quite probable that this scatter of values is explained by the fact that some crystals are intratelluric phenocrysts and, thus, xenogenic with respect to the melt that entrained them, as was suggested by Likhachev (1997).

The results of our computer simulation of phase equilibria suggest that the picritic and taxitic gabbro-dolerites could be produced by the same melt. This explains several geologic observations. First, these are traces of melt flow in the picrite unit and its gradual tapering toward the peripheral parts of the intrusion and its narrower places, which can be explained as resulting from the accumulation of denser intratelluric *Ol* phenocrysts in deeper zones of the intrusion. The uneven

distribution of these crystals caused the internal heterogeneity of the picrite unit, and its sharp boundary with the overlying olivine gabbro-dolerites can be naturally interpreted as a consequence of the practically full settling of the intratelluric phase. In this connection, it is pertinent to recall that the sharp character of the upper boundary of the picritic gabbro-dolerite unit was first obtained by the direct modeling of in-chamber differentiation of the Talnakh magma in compliance with the convection–cumulation mechanism (Dneprovskaya *et al.*, 1987).

Finally, one of the most disputable problems is the spatial distribution of taxitic and picritic gabbro-dolerites. The fact that the *Ol*-enriched and denser picritic rocks rest on less dense taxites caused the researchers of the latter to refer to it as "suspended" in the sense of the hydrodynamic instability of the system (Zolotukhin, 1997). It should be mentioned that the occurrence of a zone of MgO enrichment upward from the lower contact (the so-called S-shaped profile) resulted from an increase in the accumulation grade of settling olivine crystals at the concurrent displacement of the crystallization front in the opposite direction (March, 1989; Jaupart and Tait, 1995). A similar situation can be observed in several differentiated mafic massif. Data on the modeling of the dynamics of this process indicate that upward-directed olivine accumulation results from a decrease in the displacement velocity of this front with increasing distance from the contact (because of a decrease in the heat flow from the intrusive chamber; Frenkel' *et al.*, 1988). This conclusion is fully compatible with our geochemical thermometric data, which point to an increase in the percentage of cumulative *Ol* and *Pl* upward from the lower contact (Fig. 7). Simultaneously, a quantitative interpretation was provided for the well-known distribution profile of incompatible components (P, Ti, K, Na, Y, La, Sm, and Th) in the cross section of the Talnakh intrusion with a small minimum in the upper part of the taxitic gabbro-dolerite unit (Figs. 3, 7). According to our calculation results, this minimum corresponds to the smallest fraction of the parental magmatic liquid. Relations of this type seem to be apparent enough, but they have never been considered in other genetic models.

Comparison between the Model Melt Temperature and Data of Thermometric Studies

The calculated temperature of the parental Talnakh magma (T = 1200°C) significantly differs from the estimates obtained for other intrusions of the Noril'sk type by the homogenization of melt inclusions. For example, inclusions in pyroxenes and plagioclase from rocks of the Noril'sk-I and Chernogorskii massifs yielded temperatures of 1200–1275°C (Bulgakova, 1971). These data led Zolotukhin *et al.* (1975) to conclude that the intrusion temperatures of the parental magmas were as high as 1300–1350°C. Similar results were reported for magnesian basites from the basin of the Sukhaya Bakhta River, although the homogenization temperatures of inclusions in plagioclase were lower, 1180–1200°C (*Magnezial'nye bazity…*, 1984). Experimental studies of melt inclusions in minerals from the Talnakh intrusion point to crystallization temperatures of 1110–1140°C for *Aug* and 1120–1170°C for *Pl* (Vortsepnev, 1978), which are generally consistent with the results of simulation of phase relations in the taxitic and picritic gabbro-dolerites (Fig. 4). However, this leaves uncertain as to which solidification stage of the crystalline mush are approximated by these homogenization temperatures. In light of our analysis and the estimated temperature of the parental magma (1200°C), these temperatures seem to characterize the low-temperature postcumulus process in the evolution of the magmatic rock.

In conclusion, it is pertinent to mention attempts to utilize mineral–melt geothermometers in estimating the crystallization temperatures on the basis of the distribution coefficients of major oxides. This problem is commonly attacked with the use of equations for olivine equilibria (Roedder and Emslie, 1970; Perchuk and Vaganov, 1978)

$$\log K_i^{Ol-l} = A/T + B, \quad T = A/(\log K_i^{Ol-l} - B), \quad (4)$$

where i is MgO or FeO, and K_{MgO}^{Ol-l} and K_{FeO}^{Ol-l} are calculated from data on the composition of *Ol* crystals and their host rocks ($K_i^{Ol-l} = X_i^{Ol}/X_i^{rock}$). It is therewith implied that the whole-rock composition approximates the composition of the magmatic melt from which this olivine crystallized. There seem to be no need to explain in detail that simplifications of this kind may result in significant overestimations of the temperature, which increase, at the same composition of olivine, with the increasing content of cumulus material in a given sample [see Eq. (4)]. For example, in the case of the picritic gabbro-dolerites, temperature values of >1400°C were reported, which were enthusiastically cited by proponents of the origin of these high-Mg rocks related to the onset of liquid immiscibility. A more justified approach involves the utilization of weighted mean compositions of intrusive bodies as a model for the parental magmatic liquid. This approach yields the formation temperatures of discrete derivatives in the range of 1200–1300°C (*Magnezial'nye bazity…*, 1984). However, here, again, there is a strong probability of an overestimate in the crystallization temperature, if the intrusive magma was not overheated liquid.

The proposed technique for the reconstruction of the formation conditions of the Talnakh rocks is also based on the utilization of mineral–melt geothermometers, which provide the empirical basis of the COMAGMAT computer model. In this sense, this approach inherits and further develops traditional principles of phase equilibrium thermometry. However, in contrast to other approaches, our method does not require correlation

with the chemistry of minerals and makes it possible to interpret multiphase melt–crystal associations in terms of a diversity of intensive (temperature and compositions) and extensive (phase proportions) parameters.

CONCLUSIONS

1. The geochemical thermometry technique and the COMAGMAT computer model we used to estimate the phase and chemical parameters of the parental magma of the Talnakh intrusion and melt–crystal mixtures that gave rise to the taxitic and picritic gabbro-dolerites in the lower zone of the massif. These results point to the cotectic (*Ol* + *Pl*) nature of the Talnakh magma, which was intruded at a temperature of approximately 1200°C and contained 10–15% intratelluric phenocrysts, with the predominance of *Ol* (7–11%). The composition of the parental magmatic melt (liquid constituent of the magma) corresponded to tholeiitic ferrobasalt with somewhat elevated concentrations of MgO (~8 wt %) and K_2O (~0.7 wt %) compared with the "normal" flood basalts of the Siberian Platform. The composition of the parental melt was most similar to that of rocks produced during the late volcanic stage.

2. The composition of the parental magmatic melt was determined to correspond to the composition of the liquid that gave rise to the intercumulus materials in the rocks of the taxite and picrite units. The compositional variations of rocks from the lower part of the Talnakh intrusion can be explained as resultant from variations in the proportions of *Ol* and *Pl* intratelluric crystals and the intercumulus liquid. In light of these data, quantitative interpretation can be provided for the known profile of the distribution of incompatible elements (P, Ti, K, Na, Y, La, Sm, and Th) in the cross section of the Talnakh intrusion, with the small minimum in the upper part of the taxitic gabbro-dolerite unit corresponding to the minimum fraction of the parental magmatic liquid entrapped by these rocks. This justifies the conclusion that the taxitic and picritic gabbro-dolerites were produced by a single parental magma of the tholeiitic type, whose liquid constituent can be realistically approximated by the composition of the contact gabbro-dolerite.

ACKNOWLEDGMENTS

Primary analyses of rocks recovered by Holes KZ-1799 and KZ-1731 were provided by courtesy of V.A. Fedorenko (Central Institute of Geological Exploration for Base and Precious Metals). The authors thank A.P. Likhachev (same institute) for valuable comments, which were taken into account during the preparation of the manuscript. This study was supported by the Russian Foundation for Basic Research (project nos. 99-05-64875 and 00-05-64507).

REFERENCES

Al'meev, R.R. and Ariskin, A.A., Computer Simulation of Melt–Mineral Equilibria in a Water-Bearing Basaltic System, *Geokhimiya*, 1996, no. 7, pp. 624–636.

Ariskin, A.A., Phase Equilibria Modeling in Igneous Petrology: Use of COMAGMAT Model for Simulating Fractionation of Ferro-Basaltic Magmas and the Genesis of High-Alumina Basalt, *J. Volcanol. Geotherm. Res.*, 1999, vol. 90, pp. 115–162.

Ariskin, A.A. and Barmina, G.S., An Empirical Model for the Calculation of Spinel–Melt Equilibrium in Mafic Igneous Systems at Atmospheric Pressure: II. Fe–Ti Oxides, *Contrib. Mineral. Petrol.*, 1999, vol. 134, pp. 251–263.

Ariskin, A.A. and Barmina, G.S., *Modelirovanie fazovykh ravnovesii pri kristallizatsii bazal'tovykh magm* (Simulation of Phase Equilibria at Basalt Magma Crystallization), Moscow: Nauka, 2000.

Arndt, N.T., Czamanske, G.K., Wooden, J.L., and Fedorenko, V.A., Mantle and Crustal Contributions to Continental Flood Volcanism, *Tectonophysics*, 1993, vol. 223, pp. 39–52.

Barmina, G.S., Ariskin, A.A., and Frenkel', M.Ya., Petrochemical Types and Crystallization Conditions of Plagiodolerites in the Kronotskii Peninsula, Eastern Kamchatka, *Geokhimiya*, 1989, no. 2, pp. 192–206.

Barmina, G.S., Ariskin, A.A., Koptev-Dvornikov, E.V., and Frenkel', M.Ya., Estimation of the Compositions of Primary Cumulative Minerals in Differentiated Traps, *Geokhimiya*, 1988, no. 8, pp. 1108–1119.

Bergantz, G.W., Melt Fraction Diagrams: The Link between Chemical and Transport Models, *Rev. Mineral.*, 1990, vol. 24, pp. 239–257.

Bulgakova, E.N., Physicochemical Conditions of Formation of the Noril'sk Differentiated Trap Intrusions, in *Trappy Sibirskoi platformy i ikh metallogeniya* (Traps of the Siberian Platform and Their Metallogeny), Irkutsk: Institut zemnoi kory, 1971, pp. 36–37.

Carmichael, I.S.E. and Ghiorso, M.S., The Effect of Oxygen Fugacity on the Redox State of Natural Liquids and Their Crystallizing Phases, in *Modern Methods of Igneous Petrology: Understanding Magmatic Processes*, Nicholls, J. and Russell, J.K., Eds., *Rev. Mineral.*, 1990, vol. 24, pp. 191–212.

Chalokwu, C.I., Grant, N.K., Ariskin, A.A., and Barmina, G.S., Simulation of Primary Phase Relations and Mineral Compositions in the Partridge River Intrusion, Duluth Complex, Minnesota: Implications for the Parent Magma Composition, *Contrib. Mineral. Petrol.*, 1993, vol. 114, pp. 539–549.

Czamanske, G.K., Zen'ko, T.E., Fedorenko, V.A., *et al.*, Petrographic and Geochemical Characterization of Ore-Bearing Intrusions of the Noril'sk Type, Siberia; With Discussion of Their Origin, *Resource Geol.*, Spec. issue 1995, no. 18, pp. 1–45.

Distler, V.V., Grokhovskaya, T.L., Evstigneeva, T.L., *et al.*, *Petrologiya magmaticheskogo sul'fidnogo rudoobrazovaniya* (Petrology of Magmatic Sulfide Ore Mineralization), Moscow: Nauka, 1988.

Dneprovskaya, M.B. and Dneprovskii, N.V., Quantitative Description of Geochemical Regularities in the Structures of Geological Objects Using Random Functions, with the Talnakh Intrusion as an Example, *Geokhimiya*, 1988, no. 1, pp. 128–137.

Dneprovskaya, M.B., Frenkel', M.Ya., and Yaroshevskii, A.A., A Quantitative Model for Layering in the Talnakh Intrusion, Noril'sk Region, in *Postroenie modelei rudoobrazuyushchikh sistem* (Simulating Systems of Ore Mineralization), Novosibirsk: Nauka, 1987, pp. 96–106.

Dobretsov, N.L., Kochkin, Yu.N., Krivenko, A.P., and Kutolin, V.A., *Porodoobrazuyushchie pirokseny* (Rock-Forming Pyroxenes), Moscow: Nauka, 1971.

Dodin, D.A., Batuev, B.N., Mitenkov, G.A., and Izoitko, V.M., *Atlas porod i rud noril'skikh medno-nikelevykh mestorozhdenii* (Atlas of Rocks and Ores of the Noril'sk Copper–Nickel Deposits), Leningrad: Nedra, 1971.

Dyuzhikov, O.A., Distler, V.V., Strunin, B.M., *et al.*, *Geologiya i rudonosnost' Noril'skogo raiona* (Geology and Ore Potential of the Noril'sk Region), Moscow: Nedra, 1988.

Feoktistov, G.D., *Petrologiya i usloviya formirovaniya trappovykh sillov* (Petrology and Formation Conditions of Trap Sills), Novosibirsk: Nauka, 1978.

Frenkel', M.Ya., Ariskin, A.A., Barmina, G.S., *et al.*, Geochemical Thermometry of Igneous Rocks: Principles and Examples of Application, *Geokhimiya*, 1987, no. 11, pp. 1546–1562.

Frenkel', M.Ya., Yaroshevskii, A.A., *et al.*, *Dinamika vnutrikamernoi differentsiatsii bazitovykh magm* (Dynamics of the Chamber Differentiation of Basic Magmas), Moscow: Nauka, 1988.

Frenkel', M.Ya., Yaroshevskii, A.A., Koptev-Dvornikov, E.V., *et al.*, Crystallization Mechanism of Layering in Layered Intrusions, *Zap. Vses. Mineral. O–va*, 1985, part CXIV, issue 3, pp. 257–274.

Fudali, R.F., Oxygen Fugacities of Basaltic and Andesitic Magmas, *Geochim. Cosmochim. Acta*, 1965, vol. 29, pp. 1063–1075.

Geology and Ore Deposits of the Noril'sk Region, Proc. VII Int. Platinum Symp. with a Special Session of IGCP Project 336 "Intraplate Magmatism and Metallogeny," Moscow–Noril'sk, 1994.

Godlevskii, M.N., *Trappy i rudonosnye intruzii Noril'skogo raiona* (Traps and Ore-Bearing Intrusions of the Noril'sk Region), Moscow: Gosgeoltekhizdat, 1959.

Hawkesworth, C.J., Lightfoot, P.C., Fedorenko, V.A., *et al.*, Magma Differentiation and Mineralization in the Siberian Continental Flood Basalts, *Lithos*, 1995, vol. 34, pp. 61–81.

Hess, H.H. *et al.*, Pyroxenes of Common Mafic Magmas, *Am. Mineral.*, 1941, vol. 26, no. 9, pp. 515–535; no. 10, pp. 573–594.

Hoover, J.D., The Chilled Marginal Gabbro and Other Contact Rocks of the Skaergaard Intrusion, *J. Petrol.*, 1989, vol. 30, pp. 441–476.

Jaupart, C. and Tait, S., Dynamics of Differentiation in Magma Reservoirs, *J. Geophys. Res.*, 1995, vol. 100, pp. 17615–17636.

Korovyakov, I.A., Nelyubin, A.E., Raikova, Z.A., and Khortova, L.K., *Proiskhozhdenie noril'skikh trappovykh intruzii, nesushchikh sul'fidnye medno-nikelevye rudy* (The Origin of Noril'sk Trap Intrusions Containing Copper–Nickel Ores), Moscow: Gosgeotekhizdat, *Tr. Vses. Nauch.–Issled. Inst. Miner. Syr'ya, Novaya ser.*, 1963, issue 9.

Kutolin, V.A., *Problemy petrokhimii i petrologii bazal'tov* (Problems of the Petrochemistry and Petrology of Basalts), Moscow: Nauka, 1972.

Kuznetsov, Yu.A., Problems of Origin and Analysis of Associations of Magmatic Bodies, in *Izbrannye trudy* (Selected Works), Novosibirsk: Nauka, 1990, vol. III.

Lightfoot, P.C., Hawkesworth, C.J., Hergt, J., *et al.*, Remobilisation of the Continental Lithosphere by a Mantle Plume: Major- and Trace-Element, Sr-, Nd- and Pb-Isotope Evidence from Picritic and Tholeiitic Lavas of the Noril'sk District, Siberian Trap, Russia, *Contrib. Mineral. Petrol.*, 1993, vol. 114, pp. 171–188.

Likhachev, A.P., The Role of Leucocratic Gabbro in the Origin of Noril'sk Differentiated Intrusions, *Izv. Akad. Nauk SSSR, Ser. Geol.*, 1965, no. 12, pp. 50–66.

Likhachev, A.P., On the Crystallization Conditions of Trap Magmas in the Northwestern Part of the Siberian Platform, *Zap. Vses. Mineral. O–va*, 1977, no. 5, pp. 594–606.

Likhachev, A.P., On the Formation Conditions of Ore-bearing and Non-bearing Mafic–Ultramafic Magmas, *Dokl. Akad. Nauk SSSR*, 1978, vol. 238, no. 2, pp. 447–450.

Likhachev, A.P., Formation Conditions of Copper–Nickel Deposits, *Sov. Geol.*, 1982, no. 6, pp. 31–46.

Likhachev, A.P., Ore-bearing Intrusions of the Noril'sk Region, *Proc. Sudbury–Noril'sk Symp.*, Ontario, 1994, pp. 185–202.

Likhachev, A.P., Trap Magmatism and Platinum–Copper–Nickel Ore Mineralization in the Noril'sk District, *Otech. Geol.*, 1997, no. 10, pp. 8–19.

Lur'e, M.L., Masaitis, V.L., and Polunina, L.A., Intrusive Traps in the Western Margin of the Siberian Platform, in *Petrografiya Vostochnoi Sibiri* (The Petrography of Eastern Siberia), Moscow: Akad. Nauk SSSR, 1962, vol. 1, pp. 5–70.

Magnezial'nye bazity zapada Sibirskoi platformy i voprosy nikelenosnosti (Magnesian Basic Rocks from the Western Siberian Platform and the Problem of Nickel-Bearing Potential), Sobolev, V.S., Ed., Novosibirsk: Nauka, 1984.

Marsh, B.D., Magma Chambers, *Ann. Rev. Earth Planet. Sci.*, 1989, vol. 17, pp. 439–474.

Masaitis, V.L., Petrology of the Alamdzhakh Trap Intrusion, *Tr. Vses. Nauch.–Issled. Geol. Inst.*, 1958, vol. 22.

Naldrett, A.J., A Model for the Ni–Cu–PGE Ores of the Noril'sk Region and Its Application to Other Areas of Flood Basalt, *Econ. Geol.*, 1992, vol. 87, pp. 1945–1962.

Naldrett, A.J., Fedorenko, V.A., Asif, M., *et al.*, Controls on the Composition of Ni–Cu Sulfide Deposits as Illustrated by Those at Noril'sk, Siberia, *Econ. Geol.*, 1996, vol. 91, pp. 751–773.

Naldrett, A.J., Lightfoot, P.C., Fedorenko, V.A., *et al.*, Geology and Geochemistry of Intrusions and Flood Basalts of the Noril'sk Region, USSR, with Applications for the Origin of the Ni–Cu Ores, *Econ. Geol.*, 1992, vol. 87, pp. 975–1004.

Naslund, H.R. and McBirney, A.R., Mechanisms of Formation of Igneous Layering, *Layered Intrusions*, Cawthorn, R.G., Ed., Amsterdam: Elsevier, 1996, pp. 1–43.

Nesterenko, G.V. and Al'mukhamedov, A.I., *Geokhimiya differentsirovannykh trappov* (Geochemistry of Differentiated Traps), Moscow: Nauka, 1973.

Nesterenko, G.V., Tikhonenkov, P.I., and Romashova, T.V., Basalts of the Putorana Plateau, *Geokhimiya*, 1991, no. 10, pp. 1419–1425.

Oleinikov, B.V., *Geokhimiya i rudogenez platformennykh bazitov* (Geochemistry and Ore Genesis in Platform Basic Rocks), Novosibirsk: Nauka, 1979.

Perchuk, L.L. and Vaganov, V.I., Temperature Regime of Crystallization and Differentiation of Basic and Ultrabasic Magmas, in *Ocherki fiziko-khimicheskoi petrologii* (Essays on Physicochemical Petrology), Moscow: Nauka, 1978, issue VII, pp. 142–173.

Petrologiya i perspektivy rudonosnosti trappov severa Sibirskoi platformy (Petrology and Ore Potential of the Traps of the Northern Siberian Platform), Zolotukhin, V.V. and Vilenskii, A.M., Eds., Novosibirsk: Nauka, 1978.

Renner, J., Evans, B., and Hirth, G., On the Rheologically Critical Melt Fraction, *Earth Planet. Sci. Lett.*, 2000, vol. 181, pp. 585–594.

Roeder, P.L. and Emslie, E., Olivine–Liquid Equilibrium, *Contrib. Mineral. Petrol.*, 1970, vol. 29, pp. 275–289.

Ryabov, V.V. and Zolotukhin, V.V., *Mineraly differentsirovannykh trappov* (Minerals of Differentiated Traps), Novosibirsk: Nauka, 1977.

Ryabov, V.V., Shevko, A.Ya., and Gora, M.P., Igneous Rocks of the Noril'sk Region, in *Petrologiya trappov* (Petrology of Traps), Novosibirsk: Nonparel', 2000, vol. 1.

Sharapov, V.N., Cherepanov, A.N., Popov, V.N., and Lobov, A.G., Dynamics of Cooling of Mafic Melt Filling a Funnel-Shaped Intrusive Reservoir, *Petrologiya*, 1997, vol. 5, no. 1, pp. 10–22.

Sharma, M., Siberian Traps, in *Large Igneous Provinces. Continental, Oceanic, and Planetary Flood Volcanism*, Mahoney, J.J. and Coffin, M.F., Eds., AGU Geophys. Monogr., 1997, vol. 100, pp. 273–295.

Sinton, J., Langmuir, C., Bender, J., and Detric, R., What Is a Magma Chamber? *Ridge Events*, 1992, vol. 3, no. 1, pp. 46–48.

Sluzhenikin, S.F., Distler, V.V., Dyuzhikov, O.A., *et al.*, Low-Sulfide Platinum Ore Mineralization in the Noril'sk Differentiated Intrusions, *Geol. Rudn. Mestorozhd.*, 1994, vol. 36, no. 3, pp. 195–217.

Sobolev, A.V., The Problems of Origin and Evolution of Mantle Magmas, *Doctoral (Geol.–Min.) Dissertation*, Moscow: Vernadsky Inst. Geokhim. Analit. Khim., Akad. Nauk SSSR, 1997.

Vilenskii, A.M. and Oleinikov, B.V., The Principal Factors of Diversity and Classification Problems of Traps of the Siberian Platform, in *Geologiya i petrologiya intruzivnykh trappov Sibirskoi platformy* (Geology and Petrology of Intrusive Traps of the Siberian Platform), Moscow: Nauka, 1970, pp. 5–25.

Vortsepnev, V.V., Temperature, Pressure, and Geochemical Conditions of Formation of the Talnakh Copper–Nickel Deposit, *Cand. Sc. (Geol.–Min.) Dissertation*, Moscow: Moscow State University, 1978.

Zen'ko, T.E. and Czamanske, G.K., Special and Petrologic Aspects of the Noril'sk and Talnakh Ore Junctions, *Proc. Sudbury–Noril'sk Symp.*, Lightfoot, P.C. and Naldrett, A.J., Eds., Ontario, 1994, pp. 263–282.

Zolotukhin, V.V., Trap Magmatism and Formation Conditions of Ore-Bearing Differentiated Intrusions of the Siberian Platform, in *Trappy Sibirskoi platformy i ikh metallogeniya* (Traps of the Siberian Platform and Their Metallogeny), Irkutsk: Institut zemnoi kory, 1971, pp. 53–59.

Zolotukhin, V.V., Mafic Pegmatoids of the Noril'sk Ore-Bearing Intrusions and the Problem of Ore Mineralization of Noril'sk Type, *Tr. Ob"edin. Inst. Geol. Geofiz. Mineral.*, Novosibirsk: Sib. Otd. Ross. Akad. Nauk, 1997, issue 834.

Zolotukhin, V.V. and Laguta, O.N., On the Fractionation of Magnesian Mafic Melts and Trap Diversity of Siberian Platform, *Dokl. Akad. Nauk SSSR*, 1985, vol. 280, no. 4, pp. 967–972.

Zolotukhin, V.V., Ryabov, V.V., Vasil'ev, Yu.R., and Shatkov, V.A., *Petrologiya Talnakhskoi rudonosnoi differentsirovannoi trappovoi intruzii* (Petrology of the Talnakh Ore-Bearing Differentiated Trap Intrusion), Novosibirsk: Nauka, 1975.

Zolotukhin, V.V. and Vasil'ev, Yu.R., *Problemy platformennogo magmatizma (na primere Sibirskoi platformy)* (Problems of Platform Magmatism: Examples from the Siberian Platform), Vasilenko, B.V., Ed., Novosibirsk: Nauka, 1986.

Zotov, I.A., *Genezis trappovykh intruzivov i metamorficheskikh obrazovanii Talnakha* (The Genesis of Trap Intrusions and Metamorphic Rocks of Talnakh), Moscow: Nauka, 1979.

Zotov, I.A., *Transmagmaticheskie flyuidy v magmatizme i rudoobrazovanii* (Transmagmatic Fluids in Magmatism and Ore Mineralization), Moscow: Nauka, 1989.